

## Reduced Uranium Complexes: Synthetic and DFT Study of the Role of $\pi$ Ligation in the Stabilization of Uranium Species in a *Formal* Low-Valent State

Iliia Korobkov, Serge Gorelsky, and Sandro Gambarotta\*

Department of Chemistry, University of Ottawa, Ottawa, Ontario K1N 6N5, Canada

Received January 15, 2009; E-mail: Sandro.Gambarotta@uottawa.ca

**Abstract:** Reaction of  $\text{UCl}_4(\text{THF})_4$  with  $1,3\text{-}[2,5\text{-}(i\text{-Pr})_2\text{PhNC}(\text{=CH}_2)]_2\text{C}_6\text{H}_4\text{Li}_2$  produced a complex formulated as  $\{[1,3\text{-}[2,5\text{-}(i\text{-Pr})_2\text{PhNC}(\text{=CH}_2)]_2\text{C}_6\text{H}_4\}\text{UCl}_3[\text{Li}(\text{THF})_4]$  (**1**) that exhibits a nonagostic interaction between one of the carbon atoms of the central phenyl ring and the U metal center. This interaction leads to significant weakening of the corresponding C–H bond, thereby facilitating proton removal in consecutive transformations. Attempts to form trivalent uranium derivatives were carried out by reacting the same ligand dianion with in situ-prepared “ $\text{UCl}_3$ ”. The reaction indeed afforded a trivalent species formulated as  $\{1,3\text{-}[2,5\text{-}(i\text{-Pr})_2\text{PhNC}(\text{=CH}_2)]_2\text{C}_6\text{H}_4\}\text{U}(\mu\text{-Cl})_3[\text{Li}(\text{THF})_2]_2$  (**2**). The configuration of the ligand system in this complex is similar to that in **1**, with the same type of arrangement of the central phenyl ring. Further reduction chemistry with a variety of reagents and conditions was examined. Reaction of **1** with 1 equiv of lithium naphthalenide at 0 °C did not afford **2** but instead gave a closely related U(III) complex formulated as  $\{1,3\text{-}[2,5\text{-}(i\text{-Pr})_2\text{PhNC}(\text{=CH}_2)]_2\text{C}_6\text{H}_4\}\text{U}(\text{THF})(\mu\text{-Cl})_2[\text{Li}(\text{Et}_2\text{O})_2]$  (**3**). Both of the trivalent complexes **2** and **3** reacted thermally in boiling THF, undergoing oxidation of the metal center to afford a new tetravalent compound  $\{1,3\text{-}[2,5\text{-}(i\text{-Pr})_2\text{PhNC}(\text{=CH}_2)]_2\text{C}_6\text{H}_3\}\text{U}(\text{THF})(\mu\text{-Cl})_2[\text{Li}(\text{THF})_2]$  (**4**) in which the oxidation of the trivalent center occurred at the expense of the central phenyl ring C–H bond. Reaction of **1** with 3 equiv of lithium naphthalenide at room temperature afforded  $\{[1,3\text{-}[2,5\text{-}(i\text{-Pr})_2\text{PhNC}(\text{=CH}_2)]_2\text{C}_6\text{H}_3\}\text{U}(\mu\text{-Cl})(\mu\text{-}[\text{O}(\text{CH}_2)_3\text{CH}_2])[\text{Li}(\text{DME})][\text{Li}(\text{DME})_3]$  (**5**). In this species, the tetravalent metal center forms a six-membered metallacycle ring with a moiety arising from THF ring opening. Reaction in DME afforded reductive cleavage of the solvent accompanied by reoxidation of U to the tetravalent state. Reduction of **1** in DME with 2 equiv of potassium naphthalenide at room temperature gave a mixture of two compounds having very similar structures. The two different species  $\{[1,3\text{-}[2,5\text{-}(i\text{-Pr})_2\text{PhNC}(\text{=CH}_2)]_2\text{C}_6\text{H}_3\}\text{UCl}(\text{OCH}_3)[\text{Li}(\text{DME})_3]$  (**6a**) and  $\{[1,3\text{-}[2,5\text{-}(i\text{-Pr})_2\text{PhNC}(\text{=CH}_2)]_2\text{C}_6\text{H}_3\}\text{UCl}_2[\text{Li}(\text{DME})_3]$  (**6b**) cocrystallized in a ratio very close to 1:1 within the same unit cell. The methoxide group was generated from cleavage of the DME solvent. We also attempted the reduction of **1** with a different reducing agent such as NaH in DME. After a slow reaction, a new species formulated as  $\{1,3\text{-}[2,5\text{-}(i\text{-Pr})_2\text{PhNC}(\text{=CH}_2)]_2\text{C}_6\text{H}_3\}\text{U}(\mu\text{-OCH}_3)_3(\mu,\eta^6\text{-Na})[\eta^3\text{-Na}(\text{DME})]$  (**7**) was isolated in significant yield. Once again, the crystal structure revealed the presence of several methoxy groups coordinated to the U center in addition to the metalation of the ligand phenyl ring. To minimize solvent cleavage, reduction of **1** was also carried out at low temperature (–35 °C) and with a larger amount (4 equiv) of lithium naphthalenide. After suitable workup, the new species  $\{[1,3\text{-}[2,5\text{-}(i\text{-Pr})_2\text{PhNC}(\text{=CH}_2)]_2\text{C}_6\text{H}_3\}\text{U}\{1,3\text{-}[2,5\text{-}(i\text{-Pr})_2\text{PhN}=\text{C}(\text{CH}_3)]_2\text{C}_6\text{H}_4\}[\text{Li}(\text{DME})(\text{THF})] \cdot \text{Et}_2\text{O}$  (**8**) was isolated in significant yield. Even in this case, the uranium atom is surrounded by the expected trianionic, ring-metalated ligand. However, a second ligand unit surrounds the metal center, being bonded through a part of the  $\pi$  system. Reaction of **1** with excess NaH in toluene proceeded slowly at room temperature, affording a significant yield of  $\{[1,3\text{-}[2,5\text{-}(i\text{-Pr})_2\text{PhNC}(\text{=CH}_2)]_2\text{C}_6\text{H}_3\}\text{U}\{1,3\text{-}[2,5\text{-}(i\text{-Pr})_2\text{PhN}=\text{C}(\text{CH}_3)]_2\text{C}_6\text{H}_4\}\{\text{Na}(\text{DME})_2\}[\text{Na}(\text{DME})_3] \cdot \frac{1}{2}\text{C}_7\text{H}_8$  (**9**) after crystallization from DME/toluene. Similar to **8**, the complex still contains one ring-metalated trianionic ligand and one intact ligand that has regained the H atoms and restored the two imine functions. Although according to their connectivities, complexes **8** and **9** could be assigned with the *formal* oxidation states +2 and +1, respectively, density functional theory calculations clearly indicated that these species contain additional spin density on the ligand system with the metal center in its more standard trivalent state.

### Introduction

An extraordinary and unpredictable reactivity is the primary characteristic of low-valent complexes of *f*-block elements.<sup>1–4</sup>

There are tangible signs in the literature that outstanding chemical reactivity, along the line of that discovered for divalent lanthanides, may also be provided by reduced actinide complexes.<sup>1a,3,4</sup> For example, trivalent uranium complexes are widely established with a variety of  $\sigma$ - and  $\pi$ -donor ligand systems,<sup>5–7</sup> providing remarkable examples of dinitrogen activation/reduction<sup>5b,e,6</sup> and cleavage,<sup>7</sup> C–H bond activation,<sup>8</sup> solvent fragmentation,<sup>7,8a,9</sup> bonding of small molecules in

(1) For reviews of lanthanide reactivity, see: (a) Evans, W. J.; Davis, B. L. *Chem. Rev.* **2002**, *102*, 2119. (b) Edelmann, F. T.; Freckmann, D. M. M.; Schumann, H. *Chem. Rev.* **2002**, *102*, 1851. (c) Bochkarev, M. N. *Chem. Rev.* **2002**, *102*, 2089.

unusual bonding modes<sup>10</sup> (including a unique case of sp<sup>3</sup>-C-H bond coordination<sup>8c</sup>), and oxidative elimination of H<sub>2</sub>.<sup>4i</sup> Therefore, it is conceivable that an even higher reactivity may be expected when actinide species are further reduced. The problem with reduced actinides is that these species embark on a very substantial electron-transfer interaction with the ligand system due to an intrinsic instability of the low oxidation state. As an extreme case, even simple salts such as UI<sub>2</sub> and ThI<sub>2</sub> have been regarded as consisting of higher-valent species with *f*-spin density transferred into a sort of conduction band.<sup>11</sup> Given this tendency,  $\pi$ -bonded ligands may be particularly effective for stabilizing reduced species because they provide the possibility of electron-transfer interactions and consequent delocalization. This idea is further supported by the observation that the sole cases of paramagnetic Th(III) derivatives<sup>12</sup> have been obtained exclusively with  $\pi$ -donor ligand systems (Cp and COT) and, again, are unlikely to contain an authentic low-valent thorium.<sup>12c</sup>

Furthermore, seminal work by Cummins has shown that it is possible to prepare inverted sandwich  $\pi$ -arene complexes with the formal appearance of divalent derivatives.<sup>13</sup> Even though theoretical calculations have clearly indicated that the actual oxidation state of uranium is in fact substantially higher, the chemical reactivity remarkably remained that of a genuine two-electron reductant. Thus, the terms "low-valent synthons" and "low-valent synthetic equivalents" have been forged for these reduced species.

The behavior of thorium arenes<sup>4a,14</sup> obtained through reduction of tetravalent compounds is along the same lines. In these complexes, however, the distortion of the  $\pi$ -bonded aromatic rings that results from the presence of substantial back-bonding is very visible and clearly attributes the tetravalent state to the Th atom. Again, these species act as reactive low-valent synthons. Simple dissociation of the coordinated arene in its intact form triggers a variety of processes, including dinitrogen reduction and cleavage, solvent fragmentation, and deoxygenation.<sup>4a,15</sup>

Ligand systems that contain a large *noncoordinating*  $\pi$  system can also achieve the purpose of stabilizing a reduced species. For example, the bis(imine)pyridine ligand has shown versatility in the trapping of highly reactive units such as NdI<sub>2</sub><sup>16</sup> and AlR<sub>2</sub>.<sup>17</sup> This is possible only because this particular ligand efficiently embarks on metal-to-ligand electron transfer.<sup>17</sup> As a result, the actual oxidation state of the metal in all of these derivatives is higher. Remarkably, however, the high reactivity expected for a genuine low-valent metal center is preserved.<sup>18–21</sup>

This background prompted us to attempt the reduction of uranium complexes involving a dianionic ligand system based

- (2) For recent examples of lanthanide reactivity, see: (a) Evans, W. J.; Champagne, T. M.; Ziller, J. W.; Kaltsayannis, N. *J. Am. Chem. Soc.* **2006**, *128*, 16178. (b) Evans, W. J.; Lee, D. S.; Ziller, J. W.; Kaltsayannis, N. *J. Am. Chem. Soc.* **2006**, *128*, 14176. (c) Zimmermann, M.; Toernroos, K. W.; Anwander, R. *Angew. Chem., Int. Ed.* **2007**, *46*, 3126. (d) Edelmann, A.; Blaurock, S.; Lorenz, V.; Hilfert, L.; Edelmann, F. T. *Angew. Chem., Int. Ed.* **2007**, *46*, 6732. (e) Evans, W. J.; Champagne, T. M.; Ziller, J. W. *Organometallics* **2007**, *26*, 1204. (f) Bowman, L. J.; Izod, K.; Clegg, W.; Harrington, R. W. *Organometallics* **2007**, *26*, 2646. (g) Wiecko, M.; Roesky, P. W. *Organometallics* **2007**, *26*, 4846. (h) Roger, M.; Belkhiiri, L.; Arliguie, T.; Thuery, P.; Boucekkine, A.; Ephritikhine, M. *Organometallics* **2008**, *27*, 33. (i) Evans, W. J.; Montalvo, E.; Champagne, T. M.; Ziller, J. W.; DiPasquale, A. G.; Rheingold, A. L. *Organometallics* **2008**, *27*, 3582. (j) Meyer, G. *Angew. Chem., Int. Ed.* **2008**, *47*, 4962. (k) Amin, S. B.; Marks, T. J. *Angew. Chem., Int. Ed.* **2008**, *47*, 2006. (l) Evans, W. J.; Montalvo, E.; Champagne, T. M.; Ziller, J. W.; DiPasquale, A. G.; Rheingold, A. L. *J. Am. Chem. Soc.* **2008**, *130*, 16. (m) Evans, W. J.; Schmiege, B. M.; Lorenz, S. E.; Miller, K. A.; Champagne, T. M.; Ziller, J. W.; DiPasquale, A. G.; Rheingold, A. L. *J. Am. Chem. Soc.* **2008**, *130*, 8555.
- (3) For a review of actinide reactivity, see: Ephritikhine, M. *Chem. Rev.* **1997**, *97*, 2193.
- (4) For recent examples of actinide reactivity, see: (a) Korobkov, I.; Gambarotta, S.; Yap, G. P. A. *Angew. Chem., Int. Ed.* **2003**, *42*, 814. (b) Evans, W. J.; Kozimor, S. A.; Ziller, J. W. *Chem. Commun.* **2005**, 4681. (c) Gaunt, A. J.; Scott, B. L.; Neu, M. P. *Chem. Commun.* **2005**, *128*, 3215. (d) Roger, M.; Barros, N.; Arliguie, T.; Thuery, P.; Maron, L.; Ephritikhine, M. *J. Am. Chem. Soc.* **2006**, *128*, 8790. (e) Kiplinger, J. L.; Pool, J. A.; Schelter, E. J.; Thompson, J. D.; Scott, B. L.; Morris, D. E. *Angew. Chem., Int. Ed.* **2006**, *45*, 2036. (f) Stubbert, B. D.; Marks, T. J. *J. Am. Chem. Soc.* **2007**, *129*, 4253. (g) Minasian, S. G.; Krinsky, J. L.; Williams, V. A.; Arnold, J. J. *J. Am. Chem. Soc.* **2008**, *130*, 10086. (h) Evans, W. J.; Miller, K. A.; Ziller, J. W. *Angew. Chem., Int. Ed.* **2008**, *47*, 589. (i) Lukens, W. W., Jr.; Beshouri, S. M.; Bloesch, L. L.; Andersen, R. A. *J. Am. Chem. Soc.* **1996**, *118*, 901. (j) Karmazin, L.; Mazzanti, M.; Pécaut, J. *Inorg. Chem.* **2003**, *42*, 5900.
- (5) For example, see: (a) Korobkov, I.; Gambarotta, S.; Yap, G. P. A.; Thompson, L.; Hay, P. J. *Organometallics* **2001**, *20*, 5440. (b) Cloke, F. G.; Hitchcock, P. B. *J. Am. Chem. Soc.* **2002**, *124*, 9352. (c) Evans, W. J.; Nyce, G. W.; Forrestal, K. J.; Ziller, J. W. *Organometallics* **2002**, *21*, 1050. (d) Castro-Rodríguez, I.; Olsen, K.; Gantzel, P.; Meyer, K. J. *J. Am. Chem. Soc.* **2003**, *125*, 4565. (e) Evans, W. J.; Kozimor, S. A.; Ziller, J. W. *J. Am. Chem. Soc.* **2003**, *125*, 14264. (f) Nakai, H.; Hu, X.; Zakharov, L. N.; Rheingold, A. L.; Meyer, K. *Inorg. Chem.* **2004**, *43*, 855. (g) Castro-Rodríguez, I.; Meyer, K. J. *J. Am. Chem. Soc.* **2005**, *127*, 11242. (h) Evans, W. J.; Kozimor, S. A.; Ziller, J. W.; Fagin, A. A.; Bochkarev, M. N. *Inorg. Chem.* **2005**, *44*, 3993. (i) Gaunt, A. J.; Scott, B. L.; Neu, M. P. *Angew. Chem., Int. Ed.* **2006**, *45*, 1638. (j) Karmazin, L.; Mazzanti, M.; Bezombes, J.-P.; Gateau, C.; Pécaut, J. *Inorg. Chem.* **2004**, *43*, 5147. (k) Karmazin, L.; Mazzanti, M.; Pécaut, J. *Chem. Commun.* **2002**, 654.
- (6) (a) Cloke, F. G.; Green, J. C.; Kaltsayannis, N. *Organometallics* **2004**, *23*, 832. (b) Evans, W. J.; Lee, D. S.; Rego, D. B.; Perotti, J. M.; Kozimor, S. A.; Moore, E. K.; Ziller, J. W. *J. Am. Chem. Soc.* **2004**, *126*, 14574.
- (7) Korobkov, I.; Gambarotta, S.; Yap, G. P. A. *Angew. Chem., Int. Ed.* **2002**, *41*, 3433.
- (8) (a) Korobkov, I.; Gambarotta, S.; Yap, G. P. A. *Organometallics* **2001**, *20*, 2552. (b) Arliguie, T.; Lescoq, C.; Ventelon, L.; Leverd, P. C.; Thuery, P.; Nierlich, M.; Ephritikhine, M. *Organometallics* **2001**, *20*, 3698. (c) Castro-Rodríguez, I.; Nakai, H.; Gantzel, P.; Zakharov, L. N.; Rheingold, A. L.; Meyer, K. J. *J. Am. Chem. Soc.* **2003**, *125*, 15734. (d) Pool, J. A.; Scott, B. L.; Kiplinger, J. L. *J. Am. Chem. Soc.* **2005**, *127*, 1338. (e) Evans, W. J.; Miller, K. A.; Ziller, J. W.; DiPasquale, A. G.; Heroux, K. J.; Rheingold, A. L. *Organometallics* **2007**, *26*, 4287. (f) Graves, C. R.; Schelter, E. J.; Cantat, T.; Scott, B. L.; Kiplinger, J. L. *Organometallics* **2008**, *27*, 5371. (g) Lam, O. P.; Feng, P. L.; Heinemann, F. W.; O'Connor, J. M.; Meyer, K. J. *J. Am. Chem. Soc.* **2008**, *130*, 2806.
- (9) For example, see: (a) Avens, L. R.; Barnhart, D. M.; Burns, C. J.; McKee, S. D. *Inorg. Chem.* **1996**, *35*, 537. (b) Larch, C. P.; Cloke, F. G.; Hitchcock, P. B. *Chem. Commun.* **2008**, 82.
- (10) (a) Castro-Rodríguez, I.; Nakai, H.; Zakharov, L. N.; Rheingold, A. L.; Meyer, K. *Science* **2004**, *305*, 1757. (b) Summerscales, O. T.; Cloke, F. G.; Hitchcock, P. B.; Green, J. C.; Hazari, N. *Nature* **2006**, *311*, 829.
- (11) (a) Clark, R. J.; Corbett, J. D. *Inorg. Chem.* **1963**, *2*, 2460. (b) Scaife, D. E.; Wylie, A. W. *J. Chem. Soc.* **1964**, 5450. (c) Guggenberger, L. J.; Jacobson, R. A. *Inorg. Chem.* **1968**, *7*, 2257. (d) Stowe, K.; Tratzky, S.; Beck, H. P.; Jungmann, A.; Claessen, R.; Zimmermann, R.; Meng, G.; Steiner, P.; Huefner, S. *J. Alloys Compd.* **1997**, *246*, 101.
- (12) (a) Evans, W. J.; Miller, K. A.; Kozimor, S. A.; Ziller, J. W.; DiPasquale, A. G.; Rheingold, A. L. *Organometallics* **2007**, *26*, 3568. (b) Gilbert, T. M.; Ryan, R. R.; Sattelberger, A. P. *Organometallics* **1989**, *8*, 857. (c) Parry, J. S.; Cloke, F. G.; Coles, S. J.; Hursthouse, M. B. *J. Am. Chem. Soc.* **1999**, *121*, 6867.
- (13) (a) Diaconescu, P. L.; Arnold, P. L.; Baker, T. A.; Mindiola, D. J.; Cummins, C. C. *J. Am. Chem. Soc.* **2000**, *122*, 6108. (b) Zi, G.; Jia, L.; Werkema, E. L.; Walter, M. D.; Gottfriedsen, J. P.; Andersen, R. A. *Organometallics* **2005**, *24*, 4251.
- (14) Korobkov, I.; Gambarotta, S.; Yap, G. P. A. *Angew. Chem., Int. Ed.* **2003**, *42*, 4958.
- (15) (a) Arunachalampillai, A.; Crewdson, P.; Korobkov, I.; Gambarotta, S. *Organometallics* **2006**, *25*, 3856. (b) Korobkov, I.; Arunachalampillai, A.; Gambarotta, S. *Organometallics* **2004**, *23*, 6248. (c) Korobkov, I.; Gambarotta, S. *Organometallics* **2004**, *23*, 5379.
- (16) Sugiyama, H.; Korobkov, I.; Gambarotta, S.; Moeller, A.; Budzelaar, P. H. M. *Inorg. Chem.* **2004**, *43*, 5771.

on N donor atoms combined with a  $\pi$  system, in which the  $\pi$  ligation could be only enforced by steric vicinity. This led to the selection of the 1,3-bis(methylaryliminato)benzene ligand system, 1,3-[2,5-(*i*-Pr)<sub>2</sub>PhN=C(CH<sub>3</sub>)<sub>2</sub>C<sub>6</sub>H<sub>4</sub>],<sup>22</sup> for this particular study. We expected this ligand to preserve the established electron-storage capacity of the bis(iminato)pyridine ligand. At the same time, the replacement of the central pyridine with a regular aromatic ring was expected to either enforce  $\pi$  ligation or allow ring metalation via C–H bond activation. In this event, formation of more robust complexes resilient to further reducing conditions was anticipated. In any event, trivalent uranium was chosen as the target oxidation state, since it provides highly reactive complexes<sup>4c,5</sup> and might be used as a starting material for further reduction.

In this study, we report some unusual observations obtained during our attempts to prepare low-valent uranium complexes with the 1,3-[2,5-(*i*-Pr)<sub>2</sub>PhN=C(CH<sub>3</sub>)<sub>2</sub>C<sub>6</sub>H<sub>4</sub>]<sup>2-</sup> ligand and further reduce them.

## Experimental Section

All of the operations were performed under an inert atmosphere using standard Schlenk-type techniques or with the use of nitrogen-filled drybox. Li, NaH, K, naphthalene, and UO<sub>3</sub> were purchased from Aldrich and used as received. UCl<sub>4</sub>(THF)<sub>4</sub> was prepared by recrystallization of freshly prepared UCl<sub>4</sub><sup>23a</sup> from tetrahydrofuran (THF). Solutions of “UCl<sub>3</sub>” were prepared according to a literature procedure<sup>23b</sup> and used immediately. The bis(imino)benzene ligand 1,3-[2,5-(*i*-Pr)<sub>2</sub>PhN=C(CH<sub>3</sub>)<sub>2</sub>C<sub>6</sub>H<sub>4</sub>] was prepared according to a literature procedure<sup>22</sup> and then converted to its lithium salt using a method similar to the published procedure for the bis(imino)pyridine molecule.<sup>16</sup> All of the solvents were dried by passage through Al<sub>2</sub>O<sub>3</sub>-filled columns and degassed prior to use. Elemental analyses were performed on a PerkinElmer 2400 CHN analyzer. Data for single-crystal X-ray structure determination were collected with a Bruker diffractometer equipped with a 1K SMART CCD area detector. Deuterated solvents were purchased from C/D/N Isotopes Inc. and dried over freshly activated 4 Å molecular sieves for 7 days before use. NMR spectra were recorded at 20 °C on a Varian INOVA 500 NMR spectrometer. <sup>1</sup>H and <sup>13</sup>C chemical shifts were referenced to internal solvent resonances and are reported in parts per million relative to Me<sub>4</sub>Si.

- (17) For example, see: (a) Scott, J.; Gambarotta, S.; Korobkov, I.; Knijnenburg, Q.; De Bruin, B.; Budzelaar, P. H. M. *J. Am. Chem. Soc.* **2005**, *127*, 17204. (b) Vidyaratne, I.; Scott, J.; Gambarotta, S.; Duchateau, R. *Organometallics* **2007**, *26*, 3201.
- (18) Vidyaratne, I.; Gambarotta, S.; Korobkov, I.; Budzelaar, P. H. M. *Inorg. Chem.* **2005**, *44*, 1187.
- (19) For example, see: (a) Archer, A. M.; Bouwkamp, M. W.; Cortez, M. P.; Lobkovsky, E.; Chirik, P. J. *Organometallics* **2006**, *25*, 4269. (b) Bart, S. C.; Lobkovsky, E.; Bill, E.; Wieghardt, K.; Chirik, P. J. *Inorg. Chem.* **2007**, *46*, 7055. (c) Bart, S. C.; Bowman, A. C.; Lobkovsky, E.; Chirik, P. J. *J. Am. Chem. Soc.* **2007**, *129*, 7212. (d) Scott, J.; Vidyaratne, I.; Korobkov, I.; Gambarotta, S.; Budzelaar, P. H. M. *Inorg. Chem.* **2008**, *47*, 896. (e) Trovitch, R. J.; Lobkovsky, E.; Chirik, P. J. *J. Am. Chem. Soc.* **2008**, *130*, 11631. (f) Fernandez, I.; Trovitch, R. J.; Lobkovsky, E.; Chirik, P. J. *Organometallics* **2008**, *27*, 109. (g) Bouwkamp, M. W.; Bowman, A. C.; Lobkovsky, E.; Chirik, P. J. *J. Am. Chem. Soc.* **2006**, *128*, 3340.
- (20) (a) Gibson, V. C.; Humphries, M. J.; Tellmann, K. P.; Wass, D. F.; White, A. J. P.; Williams, D. J. *Chem. Commun.* **2001**, 2252. (b) Humphries, M. J.; Tellmann, K. P.; Gibson, V. C.; White, A. J. P.; Williams, D. J. *Organometallics* **2005**, *24*, 2039. (c) Scott, J.; Gambarotta, S.; Korobkov, I. *Can. J. Chem.* **2005**, *83*, 279.
- (21) Vidyaratne, I.; Scott, J.; Gambarotta, S.; Budzelaar, P. H. M. *Inorg. Chem.* **2007**, *46*, 7040.
- (22) Nueckel, S.; Burger, P. *Organometallics* **2000**, *19*, 3305.
- (23) (a) Moeller, T. *Inorganic Syntheses*; Maple Press: York, PA, 1957; Vol. 5. (b) Moody, D. C.; Odom, J. D. *J. Inorg. Nucl. Chem.* **1979**, *41*, 533.

**Preparation of [1,3-[2,5-(*i*-Pr)<sub>2</sub>PhN=C(CH<sub>3</sub>)<sub>2</sub>C<sub>6</sub>H<sub>4</sub>]UCl<sub>3</sub>]-[Li(THF)<sub>4</sub>] (1).** The dilithium ligand salt {1,3-[2,5-(*i*-Pr)<sub>2</sub>PhN=C(CH<sub>3</sub>)<sub>2</sub>C<sub>6</sub>H<sub>4</sub>]Li<sub>2</sub>(THF)<sub>4</sub>} (1.104 g, 1.41 mmol) was solubilized in THF (5 mL). An emerald-green solution of UCl<sub>4</sub>(THF)<sub>4</sub> (0.945 g, 1.42 mmol) in THF (7 mL) was rapidly added to the dark-orange reaction mixture. The color of the solution immediately changed to dark-brown-red, and some insoluble solid appeared. After the mixture was stirred for an additional 2 h at room temperature, the insoluble material was separated via centrifugation. The mother liquor was concentrated to 5 mL, layered with hexane (15 mL), and allowed to stand for 2 days at room temperature, after which dark-brown-red crystals of **1** were obtained (1.41 g, 1.26 mmol, 89%). Anal. Calcd (Found) for C<sub>50</sub>H<sub>74</sub>N<sub>2</sub>O<sub>4</sub>ULiCl<sub>3</sub>: C, 53.69 (53.37); H, 6.67 (6.52); N, 2.50, (2.47). <sup>1</sup>H NMR (500 MHz, benzene-*d*<sub>6</sub>, 20 °C)  $\delta$  49.72 (1H, ArH), 16.36 (6H, –CH(CH<sub>3</sub>)<sub>2</sub>), 15.39 (2H, =CH<sub>2</sub>), 13.79 (2H, –CH(CH<sub>3</sub>)<sub>2</sub>), 10.80 (6H, –CH(CH<sub>3</sub>)<sub>2</sub>), 9.94 (3H, Ar'H), 9.04 (3H, Ar'H), 2.26 (6H, –CH(CH<sub>3</sub>)<sub>2</sub>), 0.51 (16H, (–CH<sub>2</sub>–)THF), 0.35 (16H, (–CH<sub>2</sub>–)THF), –0.83 (2H, ArH), –1.70 (1H, ArH), –3.68 (2H, –CH(CH<sub>3</sub>)<sub>2</sub>), –4.05 (6H, –CH(CH<sub>3</sub>)<sub>2</sub>), –14.30 (2H, =CH<sub>2</sub>).

**Preparation of {1,3-[2,5-(*i*-Pr)<sub>2</sub>PhN=C(CH<sub>3</sub>)<sub>2</sub>C<sub>6</sub>H<sub>4</sub>]U(μ-Cl)<sub>3</sub>}-[Li(THF)<sub>2</sub>]<sub>2</sub> (2).** A solution of UCl<sub>4</sub>(THF)<sub>4</sub> (0.410 g, 0.61 mmol) in THF (10 mL) was mixed at room temperature with a THF solution of potassium naphthalenide prepared from metallic K (0.024 g, 0.62 mmol) and naphthalene (0.079 g, 0.61 mmol) in THF (10 mL). The color of the solution instantly changed to dark-red upon mixing, and a considerable amount of dark-red precipitate appeared. The reaction mixture was vigorously stirred for 20 min. A solution of dilithium ligand salt {1,3-[2,5-(*i*-Pr)<sub>2</sub>PhN=C(CH<sub>3</sub>)<sub>2</sub>C<sub>6</sub>H<sub>4</sub>]Li<sub>2</sub>(THF)<sub>4</sub>} (0.476 g, 0.61 mmol) in THF (10 mL) was added directly to the reaction mixture with vigorous stirring that continued for an additional 2 h. After that period, the insoluble material was separated by centrifugation, and the volume of the resulting solution was reduced to 5 mL under vacuum. The solution was layered with 10 mL of hexane and allowed to stand at room temperature. After 3 days, dark-red crystals of **2** were obtained (0.593 g, 0.53 mmol, 86%). Anal. Calcd (Found) for C<sub>50</sub>H<sub>74</sub>N<sub>2</sub>O<sub>4</sub>ULi<sub>2</sub>Cl<sub>3</sub>: C, 53.36 (53.32); H, 6.63 (6.54); N, 2.49 (2.49).

**Preparation of {1,3-[2,5-(*i*-Pr)<sub>2</sub>PhN=C(CH<sub>3</sub>)<sub>2</sub>C<sub>6</sub>H<sub>4</sub>]U(THF)(μ-Cl)<sub>2</sub>[Li(Et<sub>2</sub>O)<sub>2</sub>] (3).** A dark-red solution of **1** (0.300 g, 0.27 mmol) in THF (7 mL) was cooled to 0 °C and then treated with a 0 °C solution of lithium naphthalenide in THF (7 mL) prepared from Li metal (0.002 g, 0.29 mmol) and naphthalene (0.039 g, 0.30 mmol). The reaction mixture was stirred for 8 h at low temperature and then warmed to ambient temperature. The THF solvent was removed under vacuum at room temperature and replaced with diethyl ether (15 mL). Some insoluble material was separated by centrifugation. The volume of the residual solution was reduced to 7 mL, and the solution was allowed to stand in the freezer at –37 °C for 3 days, after which red crystals of **3** (0.184 g, 0.18 mmol, 67%) were obtained. Anal. Calcd (Found) for C<sub>46</sub>H<sub>70</sub>N<sub>2</sub>O<sub>3</sub>ULiCl<sub>2</sub>: C, 54.44 (54.36); H, 6.95 (6.72); N, 2.76 (2.77).

**Preparation of {1,3-[2,5-(*i*-Pr)<sub>2</sub>PhN=C(CH<sub>3</sub>)<sub>2</sub>C<sub>6</sub>H<sub>3</sub>]U(THF)(μ-Cl)<sub>2</sub>[Li(THF)<sub>2</sub>] (4).** **Method A.** A dark-red solution of **1** (0.350 g, 0.31 mmol) in THF (4 mL) was treated with a THF solution (5 mL) of potassium naphthalenide prepared from K (0.013 g, 0.33 mmol) and naphthalene (0.042 g, 0.33 mmol). When the two solutions were mixed, no significant color change was observed. Nevertheless, after the mixture was stirred for 4 h at room temperature, a small amount of light-colored insoluble material appeared in the reaction vessel as well as some brightening of the reaction mixture. The insoluble material was removed by centrifugation, and the mother liquor was concentrated to 5 mL and layered with hexanes (15 mL). Dark-brown-orange crystals of **4** were obtained after 3 days (0.178 g, 0.18 mmol, 56%). Anal. Calcd (Found) for C<sub>46</sub>H<sub>65</sub>N<sub>2</sub>O<sub>3</sub>ULiCl<sub>2</sub>: C, 54.71 (54.67); H, 6.49 (6.35); N, 2.77 (2.73). <sup>1</sup>H NMR (500 MHz, THF-*d*<sub>8</sub>, 20 °C)  $\delta$  8.56 (2H, ArH), 7.87 (1H, ArH), 7.45 (4H, Ar'H), 7.39 (2H, Ar'H), 7.33

(2H,  $-\text{CH}(\text{CH}_3)_2$ ), 7.16 (1H,  $=\text{CH}_2$ ), 7.14 (1H,  $=\text{CH}_2$ ), 3.82 (THF,  $-\text{CH}_2-$ ), 3.09 (2H,  $-\text{CH}(\text{CH}_3)_2$ ), 2.18 (1H,  $=\text{CH}_2$ ), 2.16 (1H,  $=\text{CH}_2$ ), 1.94 (THF,  $-\text{CH}_2-$ ), 1.47 (12H,  $-\text{CH}(\text{CH}_3)_2$ ), 1.44 (12H,  $-\text{CH}(\text{CH}_3)_2$ ).

**Method B.** A dark-red solution of **2** (0.350 g, 0.31 mmol) in THF (15 mL) was placed in a glass high-pressure reactor and heated to 80 °C in an oil bath. A color change occurred over a period of 6 h. A visible amount of pale-colored insoluble material gradually appeared. After the reaction mixture was cooled to room temperature, all of the insoluble material was separated by centrifugation. The residual solution was concentrated to 4 mL and layered with hexanes (15 mL). After 3 days, dark-brown-orange crystals (0.241 g, 0.24 mmol, 77%) of **4** were collected. The identity of the isolated material was confirmed by both X-ray and  $^1\text{H}$  NMR data.

**Method C.** A dark-red solution of **3** (0.350 g, 0.35 mmol) in THF (15 mL) was placed in a glass high-pressure reactor and heated to 80 °C in an oil bath. As for method B, the color of the solution became visibly lighter after 6 h of stirring. The reactor was cooled to room temperature, and a very small amount of dark-colored insoluble material was separated by centrifugation. The residual solution was concentrated to 4 mL and layered with hexanes (15 mL). Dark-brown-orange crystals of **4** were obtained after 4 days (0.272 g, 0.27 mmol, 77%). The identity of the complex was confirmed by both X-ray and  $^1\text{H}$  NMR data.

**Preparation of  $\{[1,3\text{-}[2,5\text{-}(i\text{-Pr})_2\text{PhNC}(=\text{CH}_2)]_2\text{C}_6\text{H}_3\}\text{U}(\mu\text{-Cl})(\mu\text{-}[\text{O}(\text{CH}_2)_3\text{CH}_2])[\text{Li}(\text{DME})][\text{Li}(\text{DME})_3]\}$  (**5**).** A dark-red solution of **1** (0.493 g, 0.44 mmol) in THF (4 mL) was treated with a freshly made THF solution (5 mL) of lithium naphthalenide prepared from Li (0.009 g, 1.31 mmol) and naphthalene (0.170 g, 1.33 mmol). The color of the reaction mixture did not change significantly upon mixing, but some insoluble material appeared after 2 h of stirring at room temperature. Solvent was removed from the reaction mixture, and the resulting solid residue was resuspended in dimethoxyethane (DME) (4 mL). After separation of the insoluble material by centrifugation, the resulting dark-red DME solution was layered with *n*-heptane (15 mL). Dark crystals of **5** were obtained after 3 days (0.181 g, 0.15 mmol, 34%). Anal. Calcd (Found) for  $\text{C}_{54}\text{H}_{89}\text{N}_2\text{O}_3\text{ULi}_2\text{Cl}$ : C, 54.15 (53.87); H, 7.49 (7.35); N, 2.34 (2.32).  $^1\text{H}$  NMR (500 MHz, THF- $d_8$ , 20 °C)  $\delta$  8.30 (1H, ArH), 8.24 (2H, ArH), 7.13 (4H, Ar'H), 7.03 (2H, Ar'H), 7.19 (1H,  $=\text{CH}_2$ ), 6.87 (1H,  $=\text{CH}_2$ ), 3.57 (THF,  $-\text{CH}_2-$ ), 3.39 (DME,  $-\text{CH}_2-$ ), 3.21 (DME,  $-\text{CH}_3$ ), 2.77 (4H,  $-\text{CH}(\text{CH}_3)_2$ ), 2.31 (1H,  $=\text{CH}_2$ ), 2.17 (2H, cycle,  $-\text{CH}_2-$ ), 1.97 (1H,  $=\text{CH}_2$ ), 1.73 (THF,  $-\text{CH}_2-$ ), 1.15 (24H,  $-\text{CH}(\text{CH}_3)_2$ ), 0.98 (2H, cycle,  $-\text{CH}_2-$ ),  $-4.36$  (2H, cycle,  $-\text{CH}_2-$ ),  $-6.62$  (2H, cycle,  $-\text{CH}_2-$ ).

**Preparation of the Cocrystallite of  $\{[1,3\text{-}[2,5\text{-}(i\text{-Pr})_2\text{PhNC}(=\text{CH}_2)]_2\text{C}_6\text{H}_3\}\text{UCl}(\text{OCH}_3)[\text{Li}(\text{DME})_3]$  (**6a**) and  $\{[1,3\text{-}[2,5\text{-}(i\text{-Pr})_2\text{PhNC}(=\text{CH}_2)]_2\text{C}_6\text{H}_3\}\text{UCl}_2[\text{Li}(\text{DME})_3]$  (**6b**).** A solution of **1** (0.300 g, 0.27 mmol) in DME (5 mL) was quickly mixed with a solution of potassium naphthalenide prepared from K (0.021 g, 0.54 mmol) and naphthalene (0.068 g, 0.53 mmol) in DME (5 mL). The color of the reaction mixture did not change significantly, but some light-colored precipitate appeared after 1 h of stirring at room temperature. The insoluble material was eliminated by centrifugation, and the resulting dark-brown-yellow solution was layered with *n*-heptane (20 mL). After 3 days, dark-yellow crystals of the cocrystallite **6a/6b** were collected (0.197 g, 0.17 mmol, 63%). Anal. Calcd (Found) for  $\text{C}_{50.43}\text{H}_{82.29}\text{N}_2\text{O}_{8.43}\text{ULiCl}_{1.57}$ : C, 52.56 (52.18); H, 7.20 (7.04); N, 2.43 (2.39).

**Preparation of  $\{1,3\text{-}[2,5\text{-}(i\text{-Pr})_2\text{PhNC}(=\text{CH}_2)]_2\text{C}_6\text{H}_3\}\text{U}(\mu\text{-OCH}_3)_3(\mu,\eta^6\text{-Na})[\eta^3\text{-Na}(\text{DME})]$  (**7**).** **Method A.** A solution of **1** (0.350 g, 0.31 mmol) in DME (10 mL) was placed over NaH (0.100 g, 4.17 mmol). The reaction mixture was stirred at room temperature for 7 days. The insoluble material was separated by centrifugation. The resulting solution was concentrated to 5 mL and layered with heptane (15 mL). After 4 days, the dark-orange-brown crystals of **7** (0.247 g, 0.26 mmol, 84%) that had separated out were washed with hexane and dried. Anal. Calcd (Found) for  $\text{C}_{41}\text{H}_{60}\text{N}_2\text{O}_5\text{UNa}_2$ : C, 52.11 (51.93); H, 6.40 (6.32); N, 2.96 (2.89).

$^1\text{H}$  NMR (500 MHz, THF- $d_8$ )  $\delta$  8.68 (1H, ArH), 8.21 (2H, ArH), 7.93 (1H,  $=\text{CH}_2$ ), 7.84 (1H,  $=\text{CH}_2$ ), 7.08 (4H, Ar'H), 6.93 (2H, Ar'H), 3.38 (DME,  $-\text{CH}_2-$ ), 3.22 (DME,  $-\text{CH}_3$ ), 2.90 (1H,  $=\text{CH}_2$ ), 2.73 (4H,  $-\text{CH}(\text{CH}_3)_2$ ), 2.34 (1H,  $=\text{CH}_2$ ), 2.26 (DME,  $-\text{CH}_2-$ ), 2.12 (DME,  $-\text{CH}_3$ ), 1.14 (12H,  $-\text{CH}(\text{CH}_3)_2$ ), 1.13 (12H,  $-\text{CH}(\text{CH}_3)_2$ ), 3.10 (6H,  $-\text{OCH}_3$ ),  $-4.60$  (3H,  $-\text{OCH}_3$ ).

**Method B.** A solution of **6** (0.250 g, 0.22 mmol) in DME (10 mL) was placed over NaH (0.075 g, 3.13 mmol) and stirred for 7 days. The insoluble material was then removed by centrifugation. The solution was evaporated to  $\sim 4$  mL and layered with hexane (10 mL). After 4 days, the dark-brown-orange crystals of **7** (0.102 g, 0.11 mmol, 49%) that had formed were washed with hexanes and dried. The identity of this species was confirmed by comparison of X-ray and  $^1\text{H}$  NMR data.

**Preparation of  $\{[1,3\text{-}[2,5\text{-}(i\text{-Pr})_2\text{PhNC}(=\text{CH}_2)]_2\text{C}_6\text{H}_3\}\text{U}\{1,3\text{-}[2,5\text{-}(i\text{-Pr})_2\text{PhN}=\text{C}(\text{CH}_3)_2\text{C}_6\text{H}_4]\}[\text{Li}(\text{DME})(\text{THF})]\cdot\text{Et}_2\text{O}$  (**8**).** A solution of **1** (0.500 g, 0.45 mmol) in DME (5 mL) was cooled to  $-37$  °C and treated with a cold solution ( $-37$  °C) of lithium naphthalenide [Li, 0.006 g (0.87 mmol); naphthalene, 0.116 g (0.91 mmol)]. The reaction mixture was stirred at  $-37$  °C for 2 days, during which the color of the solution gradually changed from dark-red to dark-brown. Subsequently, DME was removed in vacuo while the temperature of the reaction mixture was maintained at  $-3$  °C. The solid residue was resolubilized in cold THF (5 mL,  $-37$  °C). The insoluble material was eliminated by cold filtration, and the resulting solution was allowed to stand for 3 days at  $-37$  °C after it was layered with *n*-heptane (10 mL). The dark-colored oily substance that separated out was redissolved in cold diethyl ether (10 mL) and layered with cold *n*-heptane (10 mL). After 3 additional days at  $-37$  °C, dark-brown-red crystals of **8** were obtained (0.283 g, 0.20 mmol, 44%). Anal. Calcd (Found) for  $\text{C}_{80}\text{H}_{113}\text{N}_4\text{O}_4\text{ULi}$ : C, 66.74 (66.69); H, 7.91 (7.90); N, 3.89 (3.87).

**Preparation of  $\{[1,3\text{-}[2,5\text{-}(i\text{-Pr})_2\text{PhNC}(=\text{CH}_2)]_2\text{C}_6\text{H}_3\}\text{U}\{1,3\text{-}[2,5\text{-}(i\text{-Pr})_2\text{PhN}=\text{C}(\text{CH}_3)_2\text{C}_6\text{H}_4]\}[\text{Na}(\text{DME})_2][\text{Na}(\text{DME})_3]\cdot\frac{1}{2}\text{C}_7\text{H}_8$  (**9**).** A solution of **1** (0.500 g, 0.45 mmol) in toluene (10 mL) was stirred at room temperature in the presence of NaH (0.104 g, 4.52 mmol). During the 4 days of stirring at room temperature, the red color of the mixture gradually darkened. Toluene was removed in vacuo, and the residual solid was redissolved in DME (10 mL). A small amount of insoluble material was eliminated via centrifugation. The resulting solution was layered with hexanes (15 mL). After the diffusion was completed and no solid appeared in the crystallization vessel, the solution was cooled to  $-37$  °C and allowed to stand for 24 h at low temperature, affording dark-red crystals of **9** (0.304 g, 0.18 mmol, 40%). Anal. Calcd (Found) for  $\text{C}_{91.50}\text{H}_{139}\text{N}_4\text{O}_{10}\text{UNa}_2$ : C, 63.19 (63.03); H, 8.06 (7.92); N, 3.22 (3.19).

**Computational Details.** All of the density functional theory (DFT) calculations were performed using the Gaussian 03 package<sup>24</sup> with the PBE<sup>25</sup> exchange-correlation functional and the SDD and SDDall<sup>26</sup> effective core potential (ECP) basis sets. Calculations with these two basis sets gave nearly identical results. Tight SCF convergence criteria were used for all of the calculations. The converged wave functions were tested to confirm that they corresponded to the ground-state surface. All of the calculations for the analysis of the electronic structure, including Mulliken population analysis<sup>27</sup> and the calculation of Mayer 2- and 3-center

(24) Frisch, M. J.; et al. *Gaussian 03*, revision C.02; Gaussian, Inc: Wallingford, CT, 2004.

(25) (a) Perdew, J. P.; Burke, K.; Ernzerhof, M. *Phys. Rev. Lett.* **1996**, *77*, 3865. (b) Perdew, J. P.; Burke, K.; Ernzerhof, M. *Phys. Rev. Lett.* **1997**, *78*, 1396.

(26) Fuentealba, P.; Preuss, H.; Stoll, H.; Szentpaly, L. V. *Chem. Phys. Lett.* **1989**, *89*, 418.

(27) Mulliken, R. S. *J. Chem. Phys.* **1955**, *23*, 1833.

(28) (a) Mayer, I. *Int. J. Quantum Chem.* **1986**, *29*, 73. (b) Sannigrahi, A. B.; Kar, T. *Chem. Phys. Lett.* **1990**, *173*, 569. (c) Gorelsky, S. I.; Ghosh, S.; Solomon, E. I. *J. Am. Chem. Soc.* **2006**, *128*, 278.

bond-order indices,<sup>28a,b</sup> atomic valences,<sup>28a</sup> and populations of fragment orbitals,<sup>28c</sup> were performed using the AOMix software package.<sup>29</sup>

**X-ray Crystallography.** For all of the compounds, the results presented are the best of several data collection trials. The crystals were mounted on thin glass fibers using paraffin oil and cooled to the data collection temperature. Data were collected on a Bruker-AXS SMART 1K CCD diffractometer. Data for compounds **1**, **2**, **5**, **7**, and **8** were collected with a sequence of  $0.3^\circ$   $\omega$  scans at 0, 120, and  $240^\circ$  in  $\varphi$ . To obtain acceptable redundancy data for compounds **3**, **4**, **6**, and **9**, a sequence of  $0.3^\circ$   $\omega$  scans at 0, 90, 180, and  $270^\circ$  in  $\varphi$  was used. Initial unit-cell parameters were determined from 60 data frames collected at the different sections of the Ewald sphere. Semiempirical absorption corrections based on equivalent reflections were applied.<sup>30</sup> Systematic absences in the diffraction data set and unit-cell parameters were consistent with the following space groups: monoclinic  $P2_1/m$  for **1**; orthorhombic  $Pnma$  for **2**; triclinic  $P1$  for **3**, **4**, **6**, and **9**; and monoclinic  $P2_1/n$  for **5**, **7**, and **8**. Solutions in centrosymmetric space groups yielded chemically reasonable and computationally stable refinement results for all of the compounds. The structures were solved by direct methods, completed with difference Fourier synthesis, and refined with full-matrix least-squares procedures based on  $F^2$ . The compound molecules were located in special positions (mirror plane) in the structures of **1** and **2**. In all of the other complexes, the compound molecules were located in general positions. The structure of complex **8** represents a dimer in which the two monomeric units are related by inversion center. The carbon atoms of coordinated THF solvent molecules in **1** and **2**, coordinated diethyl ether solvent molecules in **3**, and the cocrystallized toluene solvent molecule in **9** were refined isotropically because of significant thermal motion disorder and in order to maintain an optimal data-to-parameters ratio. In every structure, all of the non-hydrogen atoms except those mentioned above were refined with anisotropic displacement coefficients. The structures of all of the complexes except **7** contain severely disordered solvent molecules, either in the lattice or coordinated to the alkali cations. This significant disorder, sometimes coupled with the low quality of the collected data sets resulting from small crystal sizes, led to the appearance of several A alerts in the check-CIF files generated by the International Union of Crystallography online check-CIF routine. Nevertheless, these disordered solvent molecules are spatially separated from the uranium-containing moieties and have no effect on either the refinement stability or the errors in bonds and distances in key fragments of the structure. All of the hydrogen atoms were treated as idealized contributions. All of the scattering factors were contained in several versions of the SHELXTL program library, with the latest version used being 6.12.<sup>31</sup>

### Description of the Crystal Structures

$\{[1,3\text{-}[2,5\text{-}(i\text{-Pr})_2\text{PhNC(=CH}_2\text{)]}_2\text{C}_6\text{H}_4\}\text{UCl}_3\}\text{[Li(THF)}_4\text{]} \text{ (1)}$ . The structure of **1** consists of an anionic metalate with an unconnected, THF-solvated lithium counterion (Figure 1). The anionic part contains the uranium metal center in a slightly distorted octahedral environment [C11–U1–Cl2 =  $173.3(1)^\circ$ , C11–U1–Cl3 =  $87.2(2)^\circ$ , Cl3–U1–Cl2 =  $86.6(2)^\circ$ , C11–U1–N1 =  $96.0(4)^\circ$ , C11–U1–N2 =  $92.1(5)^\circ$ , Cl2–U1–N1 =  $88.8(4)^\circ$ , Cl2–U1–N2 =  $88.7(4)^\circ$ ]. Five coordination sites are defined by three Cl atoms [U1–Cl1 =  $2.622(3)$  Å, U1–Cl2 =  $2.599(3)$  Å, U1–Cl3 =  $2.652(5)$  Å] and two N atoms of the ligand [U1–N1 =  $2.363(14)$  Å, U1–N2 =  $2.276(15)$  Å] (Figure 1).

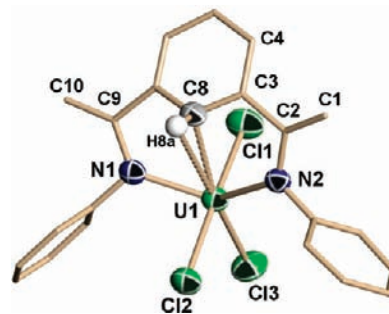


**Figure 1.** Partial thermal ellipsoid diagram of the anion of **1**, with thermal ellipsoids drawn at the 50% probability level. The isopropyl substituents on the phenyl rings have been omitted for clarity.

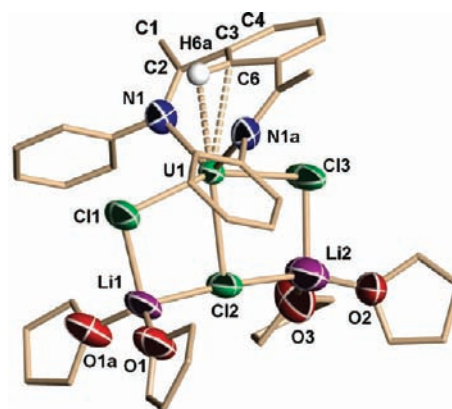


**Figure 2.** Partial thermal ellipsoid diagram of **2**, with thermal ellipsoids drawn at the 50% probability level. The isopropyl substituents on the phenyl rings have been omitted for clarity.

The sixth position is occupied by the C–H moiety of the central phenyl ring, which is coordinated side-on to the metal center and reaches a bonding contact with one of the phenyl ring carbon atoms [U1–C8 =  $2.678(12)$  Å, U1–H8a =  $3.224(12)$  Å] in what geometry-wise might be reminiscent of an agostic interaction. The dianionic character of the ligand system is apparent from the short C–C bond distances [C1–C2 =  $1.328(16)$  Å, C9–C10 =  $1.333(16)$  Å] formed by the two C atoms attached to the imino carbons as well as the fairly long C–N distances [C2–N2 =  $1.442(13)$  Å, C9–N1 =  $1.411(13)$  Å]. The central ring of the ligand is not coplanar with the rest of ligand main core [C1–C2–C3–C4 =  $41.8(18)^\circ$ ] but is not  $\pi$ -bonded to the uranium center either. A lithium cation tetrahedrally solvated by four molecules of THF [Li1–O1 =  $2.00(4)$  Å, Li1–O2 =  $2.01(4)$  Å, Li1–O3 =  $1.90(4)$  Å, Li1–O4 =  $1.85(4)$  Å] and unconnected with the anionic moiety completes the structure.

$\{[1,3\text{-}[2,5\text{-}(i\text{-Pr})_2\text{PhNC(=CH}_2\text{)]}_2\text{C}_6\text{H}_4\}\text{U}(\mu\text{-Cl)}_3\text{[Li(THF)}_2\text{)]}_2 \text{ (2)}$ . The structure of **2** shows the uranium metal center in a symmetry-generated distorted octahedral coordination environment (Figure 2). Similarly to **1**, three of the four equatorial positions are occupied by chlorine atoms [U1–Cl1 =  $2.757(3)$  Å, U1–Cl2 =  $2.880(3)$  Å, U1–Cl3 =  $2.751(3)$  Å, Cl1–U1–Cl2 =  $78.02(9)^\circ$ , Cl1–U1–Cl3 =  $154.57(10)^\circ$ ]. Two nitrogen atoms of the bis(imino) ligand reside in axial positions of the distorted octahedron [U1–N1 =  $2.402(7)$  Å, N1–U1–N1a =  $118.8(3)^\circ$ ]. The last equatorial position is occupied by one C atom of the central phenyl ring [U1–C6 =  $2.769(9)$  Å, U1–H6a =  $2.529(9)$  Å, N1–U1–C6 =  $61.95(17)^\circ$ ], with a short contact in the U–C  $\sigma$ -bonding range. The molecule is bisected by a mirror plane containing the metal center and the chlorine atoms. The dianionic nature of the ligand is apparent from the values of

(29) (a) Gorelsky, S. I.; Lever, A. B. P. *J. Organomet. Chem.* **2001**, *635*, 187. (b) Gorelsky, S. I. *AOMix*, version 6.36; University of Ottawa: Ottawa, ON, 2008.

(30) Blessing, R. *Acta Crystallogr.* **1995**, *A51*, 33.

(31) Sheldrick, G. M. *SHELXTL Program Library*; Bruker AXS: Madison, WI, 2001.

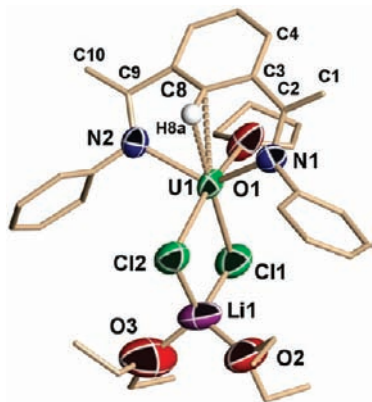


**Figure 3.** Partial thermal ellipsoid diagram of **3**, with thermal ellipsoids drawn at the 50% probability level. The isopropyl substituents on the phenyl rings have been omitted for clarity.

the C–C distances formed by the terminal carbon atoms and the C–N distances of the former imine functions [C1–C2 = 1.342(13) Å, C2–N1 = 1.381(11) Å]. As in complex **1**, the interaction of the metal center with the phenyl ring C–H bond causes a significant deviation of the ligand  $\pi$  system from planarity [C1–C2–C3–C4 = 40.3(2)°]. The three chlorine atoms bridge in pairs two Li cations [C11–Li1 = 2.38(2) Å, C12–Li1 = 2.39(2) Å, C12–Li2 = 2.41(3) Å, C13–Li2 = 2.44(3) Å]. Each Li atom resides in a tetrahedral arrangement, with two positions occupied by chlorines [C11–Li1–C12 = 96.2(7)°, C12–Li2–C13 = 91.9(11)°] and the other two by coordinated THF molecules [O1–Li1 = 1.888(13) Å, O2–Li2 = 1.67(3) Å, O3–Li2 = 2.06(3) Å, C11–Li1–O1 = 107.4(9)°, O1–Li1–O1a = 117.2(11)°, C12–Li2–O2 = 134.1(12)°, O2–Li2–O3 = 105.4(19)°]. Two of the THF molecules around a given Li atom are disordered over two positions with approximately equal occupancies.

**{1,3-[2,5-(*i*-Pr)<sub>2</sub>PhNC(=CH<sub>2</sub>)<sub>2</sub>C<sub>6</sub>H<sub>4</sub>]U(THF)( $\mu$ -Cl)<sub>2</sub>[Li(Et<sub>2</sub>O)<sub>2</sub>]} (3).** Complex **3** consists of a uranium metal center in a distorted octahedral arrangement very similar to those of **1** and **2** (Figure 3). The coordination of the metal center is defined by two nitrogens placed in the two axial positions [U1–N1 = 2.393(10) Å, U1–N2 = 2.390(10) Å, N1–U1–N2 = 123.4(3)°]. Three of the four equatorial positions are defined by two chlorine atoms [U1–Cl1 = 2.759(4) Å, U1–Cl2 = 2.720(4) Å, Cl1–U1–Cl2 = 80.28(13)°, N1–U1–Cl1 = 117.0(3)°] and the oxygen atom of a coordinated THF molecule [U1–O1 = 2.529(9) Å, Cl1–U1–O1 = 78.03(3)°, N1–U1–O1 = 96.9(4)°]. The same short contact between the metal center and the C–H bond of the phenyl ring as observed in **1** and **2** is also present in **3** and occupies the last equatorial position [U1–C8 = 2.756(13) Å, U1–H8a = 2.456(14) Å, C8–U1–Cl1 = 158.7(3)°, C8–U1–N1 = 63.6(4)°]. In perfect analogy with the two complexes above, the dianionic nature of the ligand is confirmed by the values of the C–C and C–N bond distances [C1–C2 = 1.335(19) Å, C9–C10 = 1.350(18) Å, C2–N1 = 1.407(17) Å, C9–N2 = 1.373(16) Å]. Also very comparable is the deviation of the ligand from planarity [C1–C2–C3–C4 = 36.3(5)°].

Both chlorine atoms bridge the uranium center to lithium [Li1–Cl1 = 2.36(3) Å, Li1–Cl2 = 2.34(3) Å, Cl1–Li1–Cl2 = 97.2(9)°]. The tetrahedral coordination environment of the Li cation is completed by the oxygen atoms of two coordinated molecules of diethyl ether [Li1–O2 = 1.92(4) Å, Li1–O3 = 1.96(4) Å, O2–Li1–O3 = 108.7(14)°, Cl1–Li1–O2 = 115.5(17)°].

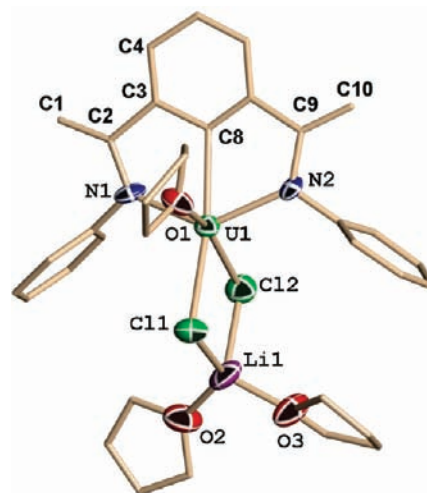


**Figure 4.** Partial thermal ellipsoid diagram of **4**, with thermal ellipsoids drawn at the 50% probability level. The isopropyl substituents on the phenyl rings have been omitted for clarity.

**{1,3-[2,5-(*i*-Pr)<sub>2</sub>PhNC(=CH<sub>2</sub>)<sub>2</sub>C<sub>6</sub>H<sub>3</sub>]U(THF)( $\mu$ -Cl)<sub>2</sub>[Li(THF)<sub>2</sub>]} (4).** The structure of **4** shows that the ligand is coordinated to the uranium center in a tridentate fashion and arranged meridionally (Figure 4). Two of the three positions are defined by the two amido nitrogen donor atoms [U1–N1 = 2.241(10) Å, U1–N2 = 2.273(10) Å, N1–U1–N2 = 132.4(4)°]. The third position is occupied by the metalated carbon atom of the central phenyl ring [U1–C8 = 2.388(13) Å, N1–U1–C8 = 66.4(4)°]. The polyanionic character of the ligand is confirmed by the C–C and C–N bond distances [C1–C2 = 1.38(2) Å, C9–C10 = 1.34(2) Å, C2–N1 = 1.41(2) Å, C9–N2 = 1.38(2) Å]. The ring metalation is responsible for the restoration of the ligand planarity [C1–C2–C3–C4 = 9.0(2)°]. The last equatorial position is occupied by one of the two chlorine atoms [U1–Cl1 = 2.792(3) Å, Cl1–U1–N1 = 115.3(3)°, Cl1–U1–C8 = 160.6(3)°]. The second chlorine atom fills the first axial position of the distorted octahedron [U1–Cl2 = 2.665(4) Å, Cl1–U1–Cl2 = 80.05(12)°, Cl2–U1–C8 = 119.3(3)°]. The second axial position is occupied by the O atom of a coordinated THF solvent molecule [U1–O1 = 2.477(9) Å, O1–U1–Cl2 = 158.5(2)°, O1–U1–C8 = 81.9(4)°]. Both chlorine atoms bridge uranium and lithium, defining two positions of the tetrahedral environment around the Li cation [Li1–Cl1 = 2.35(3) Å, Li1–Cl2 = 2.44(3) Å, Cl1–Li1–Cl2 = 94.3(9)°]. Two THF solvent molecules complete the coordination geometry of the alkali cation [Li1–O2 = 1.84(3) Å, Li1–O3 = 1.90(3) Å, O2–Li1–O3 = 109.8(13)°, Cl1–Li1–O2 = 111.4(14)°].

**{[1,3-[2,5-(*i*-Pr)<sub>2</sub>PhNC(=CH<sub>2</sub>)<sub>2</sub>C<sub>6</sub>H<sub>3</sub>]U( $\mu$ -Cl)( $\mu$ -[O(CH<sub>2</sub>)<sub>3</sub>CH<sub>2</sub>]-[Li(DME)]][Li(DME)<sub>3</sub>]} (5).** Complex **5** is ionic, with a uranium-containing anionic moiety and a solvated lithium counteranion. The uranium center adopts the usual distorted octahedral arrangement (Figure 5). Similar to complex **4**, the ligand is tridentate and meridionally arranged, with metalation of the central aromatic ring. One equatorial coordination site is occupied by a  $\sigma$ -bonded C atom [U1–C8 = 2.419(12) Å] from the central phenyl ring, while the two nitrogen atoms of the bis(amido) ligand occupy two other equatorial sites [U1–N1 = 2.391(11) Å, U1–N2 = 2.372(11) Å, N1–U1–N2 = 129.78(7)°]. One of the axial sites is occupied by a chlorine atom [U1–Cl1 = 2.846(4) Å, C35–U1–Cl1 = 153.48(6)°]. The last two coordination sites, one equatorial and one axial, are occupied by the oxygen [U1–O1 = 2.244(9) Å, O1–U1–C8

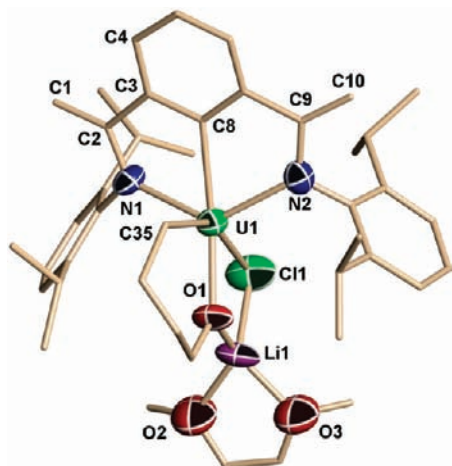


**Figure 5.** Partial thermal ellipsoid diagram of the anion of **5**, with thermal ellipsoids drawn at the 50% probability level.

= 157.86(6)°] and carbon atoms [U1–C35 = 2.476(13) Å, C35–U1–O1 = 78.91(6)°, C35–U1–C8 = 79.756(6)°], respectively, of what appears to be the result of THF ring opening (Figure 5). The ene-bis(amido) ligand adopts a nearly flat conformation having both amido residues coplanar with the metalated phenyl ring. The bond distances formed by the ene carbon atoms [(C1–C2 = 1.34(2) Å, C9–C10 = 1.358(18) Å, C2–N1 = 1.415(17) Å, C9–N2 = 1.372(17) Å] confirm the presence of the C–C double bonds and are in agreement with those of all the other complexes described above. The oxygen atom of the cleaved THF molecule and the chlorine atom bridge uranium to the Li cation [Li1–O1 = 1.89(3) Å, Li1–Cl1 = 2.30(3) Å]. The remaining two coordination sites of the coordination tetrahedron of the Li atom are filled by the two oxygen atoms of a DME molecule [Li1–O2 = 1.97(3) Å, Li1–O3 = 1.94(3) Å]. The unconnected countercation consists of a second Li cation octahedrally coordinated by six oxygen atoms from three DME molecules [Li2–O4 = 2.30(3) Å, Li2–O5 = 1.97(4) Å, Li2–O6 = 2.08(3) Å, Li2–O7 = 2.12(3) Å, Li2–O8 = 2.11(4) Å, Li2–O9 = 2.18(3) Å].

**Cocrystallite of**  $\{[1,3\text{-}[2,5\text{-}(i\text{-Pr})_2\text{PhNC(=CH}_2\text{)}]_2\text{C}_6\text{H}_3\}\text{UCl(OCH}_3\text{)}\}[\text{Li(DME)}_3]$  (**6a**) and  $\{[1,3\text{-}[2,5\text{-}(i\text{-Pr})_2\text{PhNC(=CH}_2\text{)}]_2\text{C}_6\text{H}_3\}\text{UCl}_2\}[\text{Li(DME)}_3]$  (**6b**). The structure of the cocrystallite of **6a** and **6b** consists of two chemically different but crystallographically very similar compounds cocrystallized within the same unit cell. The difference between the two species consists of the replacement of the OCH<sub>3</sub> group of **6a** with a second Cl in **6b** (Figure 6a,b). In both cases, the structure contains an anionic fragment with a heptacoordinated (pentagonal bipyramidal) U metal center and an unconnected Li countercation solvated by DME. The coordination sphere of the U atom is defined by the planar ligand, which occupies three equatorial coordination sites using two nitrogen atoms and one carbon atom of the deprotonated phenyl ring [U1–N1 = 2.395(6) Å, U1–N2 = 2.381(6) Å, U1–C8 = 2.412(7) Å, N1–U1–N2 = 132.3(2)°]. The last two equatorial positions are occupied by the two oxygen atoms of a DME molecule [U1–O2 = 2.810(6) Å, U1–O3 = 2.844(7) Å, O2–U1–O3 = 57.5(2)°, O2–U1–N1 = 84.6(3)°, O3–U1–C8 = 150.3(3)°]. A chlorine atom resides in one axial position of the coordination polyhedron [U1–Cl1 = 2.668(2) Å, C8–U1–Cl1 = 111.5(3)°]. The other axial coordination site is partly occupied by the oxygen atom of the methoxy group in the case of **6a** [U1–O1 = 1.976(16) Å, O1–U1–C8 =

95.3(3)°] and by the second chlorine atom in **6b** [U1–Cl2 = 2.628(7) Å, Cl2–U1–C8 = 90.0(3)°].

The overall **6a/6b** ratio was determined to be 43:57 on the basis of the best crystallographic refinement of thermal parameters. The cationic fragment consists of a Li atom in an octahedral coordination arrangement defined by the oxygen atoms of three DME molecules [Li2–O4 = 2.085(18) Å, Li2–O5 = 2.229(17) Å, Li2–O6 = 2.114(16) Å, Li2–O7 = 2.210(18) Å, Li2–O8 = 2.070(17) Å, Li2–O9 = 2.169(16) Å].

**{[1,3-[2,5-(i-Pr)<sub>2</sub>PhNC(=CH<sub>2</sub>)]<sub>2</sub>C<sub>6</sub>H<sub>3</sub>}U(μ-OCH<sub>3</sub>)<sub>3</sub>(μ,η<sup>6</sup>-Na)-[η<sup>3</sup>-Na(DME)]** (**7**). The structure of **7** consists of a symmetry-generated dimer (Figure 7). Each monomeric unit contains a uranium metal center in a distorted octahedral environment. The ligand exhibits the usual tridentate bonding mode by bonding the metal center through the N atoms and the C atom of the metalated central phenyl ring [C1–C2–C3–C4 = 20.1(17)°, U1–N1 = 2.440(8) Å, U1–N2 = 2.418(8) Å, U1–C8 = 2.468(10) Å, N1–U1–N2 = 130.3(3)°, N1–U1–C8 = 65.2(3)°]. The trianionic character of the ligand is indicated by the corresponding C–C and C–N bond distances as well as by the bonding contact between the uranium metal center and the carbon atom of the ligand central phenyl ring [C1–C2 = 1.316(13) Å, C9–C10 = 1.355(15) Å, N1–C2 = 1.401(12) Å, C9–N2 = 1.405(13) Å, U1–C8 = 2.468(10) Å]. The remaining equatorial and axial positions of the octahedron are filled by three CH<sub>3</sub>O groups [U1–O1 = 2.178(7) Å, U1–O2 = 2.296(6) Å, U1–O3 = 2.207(6) Å, O1–U1–O2 = 159.8(3)°, O1–U1–O3 = 89.8(3)°, O3–U1–C8 = 171.3(3)°].

Each of the three methoxy groups bridges U to one of the two Na metal centers. The first Na atom is bonded to one methoxy group [Na1–O1 = 2.296(9) Å], a portion of the central aromatic ring of the ligand [Na1–C3 = 2.844(13) Å, Na1–C7 = 3.060(12) Å, Na1–C8 = 2.583(11) Å, O1–Na1–C8 = 80.8(3)°], and the two oxygens of one DME molecule [Na1–O4 = 2.259(16) Å, Na1–O5 = 2.315(16) Å, O4–Na1–O5 = 68.3(6)°, O4–Na1–C8 = 136.0(6)°]. The second is instead bonded to the other two methoxy groups [Na2–O2 = 2.316(7) Å, Na2–O3 = 2.328(8) Å, O2–Na2–O3 = 73.8(2)°]. Additional bonding interactions are realized through methoxy group of a second identical unit [Na2–O2a = 2.402(8) Å, O2–Na2–O2a = 97.5(2)°] as well as one of the peripheral phenyl rings of the second unit [Na2–centroid(1a) = 2.578(9) Å, O2–Na2–centroid(1a) = 129.8(3)°], thereby assembling the dinuclear structure.

**{[1,3-[2,5-(i-Pr)<sub>2</sub>PhNC(=CH<sub>2</sub>)]<sub>2</sub>C<sub>6</sub>H<sub>3</sub>}U{[1,3-[2,5-(i-Pr)<sub>2</sub>PhN=C(CH<sub>3</sub>)<sub>2</sub>C<sub>6</sub>H<sub>4</sub>]}[Li(DME)(THF)]}·Et<sub>2</sub>O** (**8**). Complex **8** contains a uranium metal center surrounded by two ligands in an overall severely distorted heptacoordinate environment (Figure 8). Three sites are occupied by two nitrogen atoms and one carbon atom of one ring-metalated ligand system [U1–N1 = 2.372(4) Å, U1–N2 = 2.371(4) Å, U1–C8 = 2.420(5) Å, N1–U1–N2 = 130.60(14)°, N1–U1–C8 = 66.32(17)°]. This ligand appears to be trianionic according to the C–C and C–N bond distances [U1–C8 = 2.420(5) Å, C1–C2 = 1.342(8) Å, C9–C10 = 1.348(7) Å, C2–N1 = 1.413(6) Å, C9–N2 = 1.402(6) Å] as well as the planar configuration [N1–U1–C8–C7 = 174.0(4)°, N2–U1–C8–C3 = 178.6(4)°]. A second ligand is also bonded to uranium, affording a diene-type η<sup>4</sup> interaction with the part of the extended π system encompassing one imino function and part of the central aromatic ring [U1–N3 = 2.260(4) Å, U1–C40 = 2.682(5) Å, U1–C41 = 2.808(5) Å, U1–C43 = 2.678(5) Å, η<sup>4</sup>-centroid–U1–C8 = 165.26(17)°, η<sup>4</sup>-centroid–U1–N1 = 115.80(16)°]. In fact, the two imino functions

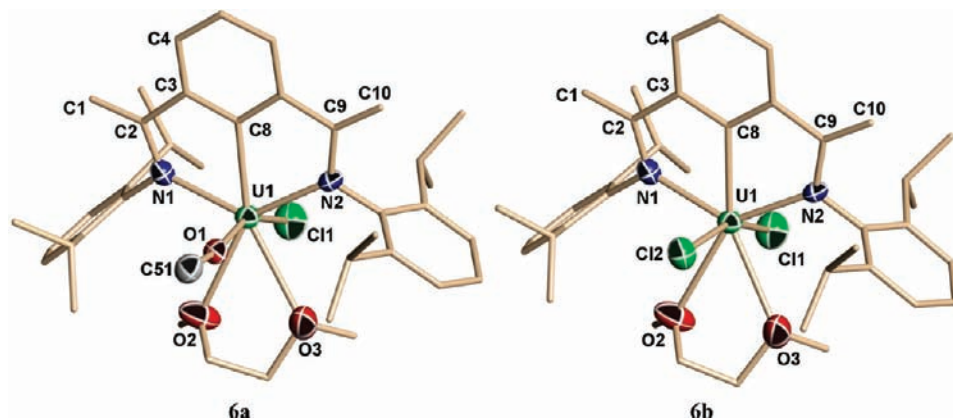


**Figure 6.** Partial thermal ellipsoid diagrams of the anions in (left) **6a** and (right) **6b**, with thermal ellipsoids drawn at the 50% probability level.

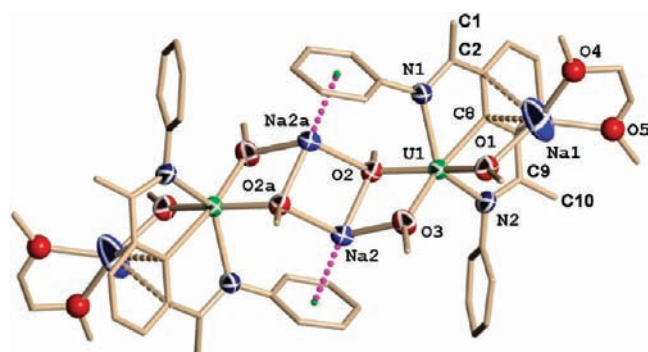


**Figure 7.** Partial thermal ellipsoid diagram of **7**, with thermal ellipsoids drawn at the 50% probability level. The isopropyl substituents on the phenyl rings have been omitted for clarity.

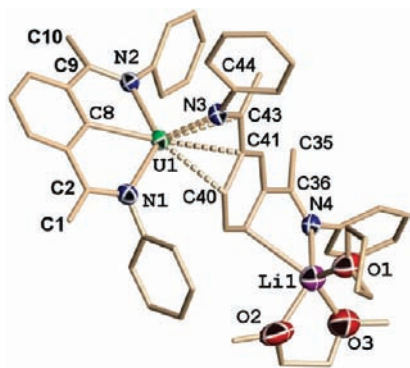


**Figure 8.** Partial thermal ellipsoid diagram of **8**, with thermal ellipsoids drawn at the 50% probability level. The isopropyl substituents on the phenyl rings have been omitted for clarity.

have been restored and the terminal carbon atom has been protonated in this second ligand system [C35–C36 = 1.502(7) Å, C43–C44 = 1.508(7) Å, C36–N4 = 1.292(6) Å, C43–N3 = 1.425(6) Å].

The structure is completed by one Li cation in a square-pyramidal arrangement coordinated to the second part of the same extended  $\pi$  system of the second, formally neutral, ligand unit [Li1–N4 = 2.120(11) Å, Li1–C38 = 2.713(12) Å]. One disordered molecule of THF and one of DME complete the coordination geometry of the alkali metal ion [Li1–O2 = 2.083(12) Å, Li1–O3 = 2.119(12) Å, O2–Li1–N4 = 109.3(5)°, O2–Li1–C38 = 153.4(5)°, O3–Li1–C38 = 90.7(4)°, Li1–O1 = 2.120(11) Å, O1–Li1–N4 = 109.3(5)°, O1–Li1–O2 =

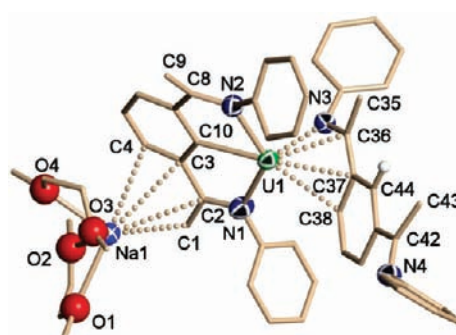


**Figure 9.** Partial thermal ellipsoid diagram of **9**, with thermal ellipsoids drawn at the 50% probability level. The isopropyl substituents on the phenyl rings have been omitted for clarity.

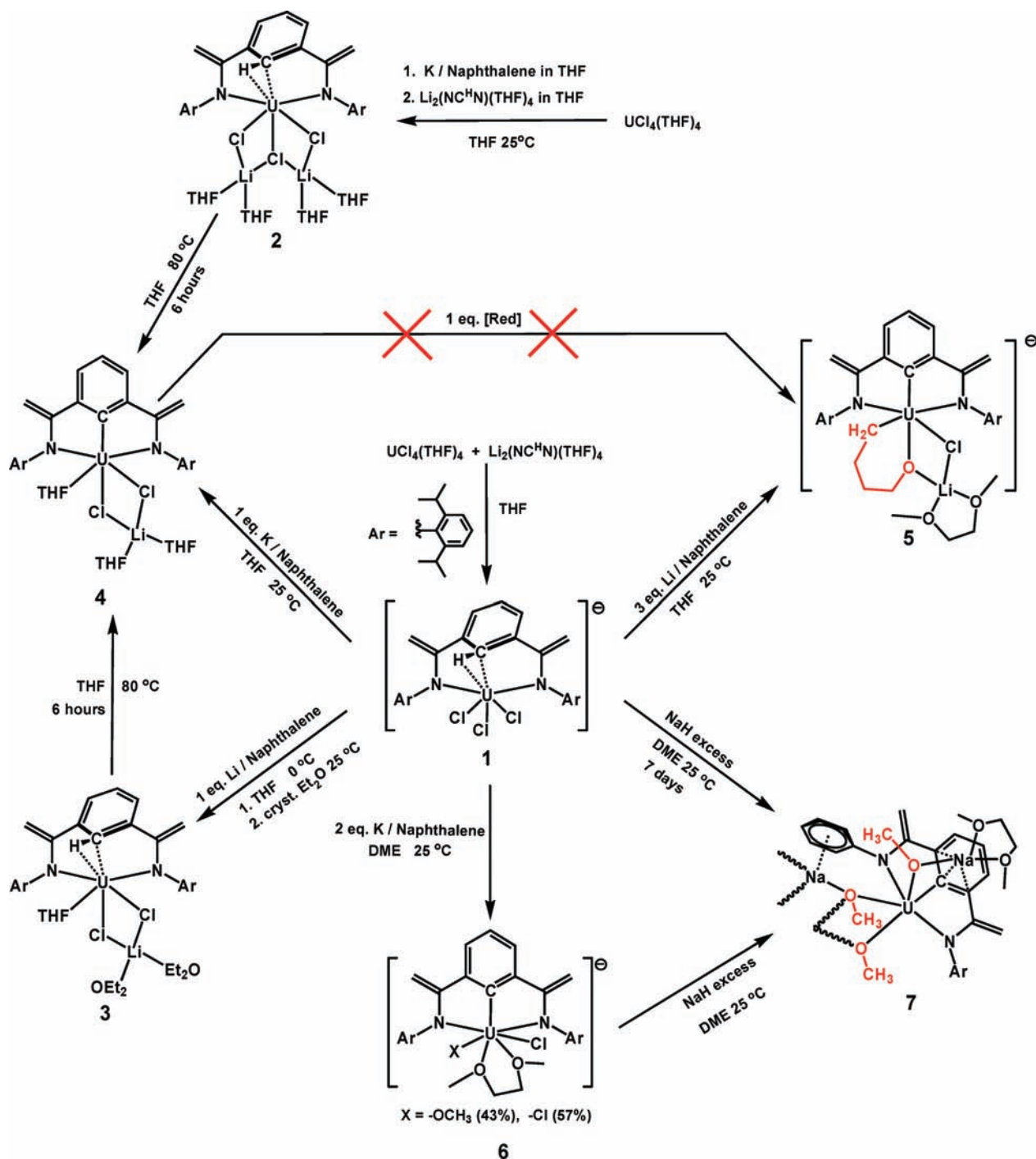
107.8(5)°. One noncoordinated molecule of diethyl ether solvent per uranium complex completes the structure.

{[1,3-[2,5-(*i*-Pr)<sub>2</sub>PhNC(=CH<sub>2</sub>)<sub>2</sub>C<sub>6</sub>H<sub>3</sub>]U{1,3-[2,5-(*i*-Pr)<sub>2</sub>PhN=C(CH<sub>3</sub>)<sub>2</sub>C<sub>6</sub>H<sub>4</sub>}{Na(DME)<sub>2</sub>}[Na(DME)<sub>3</sub>]}·<sup>1</sup>/<sub>2</sub>C<sub>7</sub>H<sub>8</sub> (**9**). The structure of **9** reveals two ligands attached to one U metal center in an arrangement strikingly similar to that observed for **8** (Figure 9). An analysis of the bond distances around C2 and C9 in the first ligand system in comparison to the corresponding bond distances around C36 and C42 in the second ligand system suggests that the first molecule has retained the trianionic bis(amido) configuration of the starting material [C2–C1 = 1.382(16) Å, C2–N1 = 1.409(14) Å, C9–C10 = 1.321(15) Å, C9–N2 = 1.378(14) Å] while the second ligand instead has gained three hydrogen atoms to become a neutral bis(imine) [C36–C35 = 1.505(14) Å, C36–N3 = 1.414(12) Å, C42–C43 = 1.521(16) Å, C42–N4 = 1.286(13) Å]. The uranium metal center is sited in a distorted trigonal-bipyramidal coordination polyhedron.

The two axial positions are occupied by two nitrogen atoms of the first [bis(amido)] ligand system [U1–N1 = 2.519(8) Å, U1–N2 = 2.359(8) Å, N1–U1–N2 = 129.5(3)°], while the carbon atom of the central phenyl ring occupies one equatorial position [U1–C8 = 2.479(11) Å, N1–U1–C8 = 64.7(3)°]. Two other equatorial positions are engaged in an interaction with the second ligand molecule. This molecule is connected to the metal center through the  $\eta^4$ -diene type of  $\pi$  bonding of one of the imino groups [U1–N3 = 2.325(8) Å, U1–C36 = 2.654(10) Å, N3–U1–N1 = 106.6(3)°] as well as one aromatic bond of the central phenyl ring [U1–C37 = 2.846(10) Å, U1–C38 = 2.790(10) Å, C38–U1–C8 = 148.2(3)°]. A sodium countercation solvated by two molecules of DME [Na1–O1 = 2.597(12) Å, Na1–O2 = 2.616(12) Å, Na1–O3 = 2.487(18) Å, Na1–O4 = 2.549(14) Å] is also part of the structure, as it bonds in  $\eta^4$ -diene fashion through the  $\pi$  system encompassing one double bond



Scheme 1



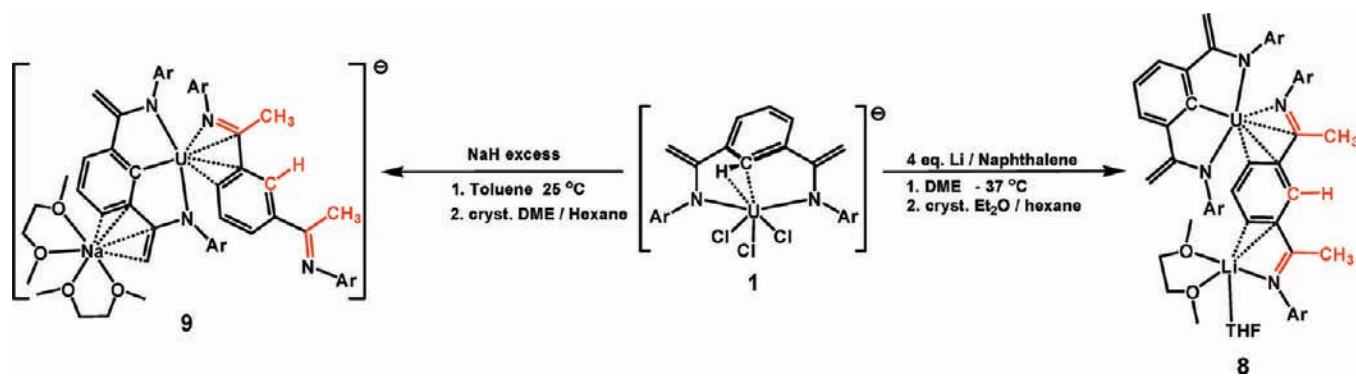
[C1–C2 = 1.382(16) Å] and an aromatic bond of the central phenyl ring [C3–C4 = 1.396(15) Å, Na1–C1 = 3.015(15) Å, Na1–C2 = 3.280(15) Å, Na1–C3 = 3.276(16) Å, Na1–C4 = 3.157(16) Å] of the triply deprotonated ligand. One additional Na counteraction ensures the electroneutrality of the structure. This Na atom resides in an octahedral environment defined by six oxygen atoms of three DME solvent molecules. [Na2–O5 = 2.445(19) Å, Na2–O6 = 2.405(17) Å, Na2–O7 = 2.372(13) Å, Na2–O8 = 2.388(14) Å, Na2–O9 = 2.355(13) Å, Na2–O10 = 2.389(12) Å]. One toluene solvent molecule in the lattice with partial occupancy of 50%, completes the structure.

## Results and Discussion

The reaction of the dianion [1,3-[2,5-(*i*-Pr)<sub>2</sub>PhNC(=CH<sub>2</sub>)<sub>2</sub>]<sub>2</sub>-C<sub>6</sub>H<sub>4</sub>]<sup>2-</sup> with  $\text{UCl}_4(\text{THF})_4$  afforded the corresponding tetravalent

uranium complex  $[\{1,3\text{-}[2,5\text{-}(i\text{-Pr})_2\text{PhNC(=CH}_2\text{)}_2\text{C}_6\text{H}_4\}\text{UCl}_3\text{-}[\text{Li}(\text{THF})_4]\text{ (I)}$  (Scheme 1). The ligand system did not adopt the anticipated  $\pi$ -bonding mode (Figure 1). The main interaction between uranium and the aromatic ring appears to be realized through only the central C atom of the phenyl ring, without any significant contributions from the corresponding C–H bond. The presence of this unconventional interaction is fully supported by the results of the DFT calculations (see below) and possibly indicates a partial charge transfer from the tetravalent uranium center to a portion of the aromatic ring. Furthermore, the interaction of the U metal center with the C atom of the ring promotes a noticeable weakening of the corresponding C–H bond (see Electronic Structures, below), which makes the

Scheme 2



aromatic ring incline toward direct metalation. In spite of the fact that the geometrical parameters of the U–C–H arrangement are similar to those observed for the coordination of cyclohexane to a U(III) metal center,<sup>8c</sup> it appears that no significant agostic interaction is present in this case.

The <sup>1</sup>H NMR spectrum of **1** is characterized by a large spreading of 16 fairly sharp lines over the range +50 to –14 ppm. Besides the two resonances of the THFs coordinated to Li, which reside approximately in the expected regions, the other resonances could not be assigned conclusively. One of the few clearly recognizable features was the C–H hydrogen of the central C atom of the central phenyl ring. Because of the close proximity of paramagnetic U metal center, the signal of this hydrogen was located at +49.72 ppm and coupled to a broad carbon resonance at –0.25 ppm. Also clearly recognizable were the =CH<sub>2</sub> hydrogens, which gave two resonances at +13.79 and –14.30 coupled to the same carbon at 134.61 ppm.

The behavior of this ligand system vis-à-vis the trivalent state of uranium was examined by reacting the same ligand dianion with in situ prepared “UCl<sub>3</sub>” (Scheme 1). The reaction indeed afforded a trivalent species formulated as {1,3-[2,5-(*i*-Pr)<sub>2</sub>PhNC(=CH<sub>2</sub>)<sub>2</sub>C<sub>6</sub>H<sub>4</sub>}U(μ-Cl)<sub>3</sub>[Li(THF)<sub>2</sub>]<sub>2</sub> (**2**) (Figure 2). The configuration of the ligand system in this complex is similar to that in **1**, with the same type of arrangement of the central phenyl ring (Figure 2). The slight increase in the bond distances formed by the uranium metal center as well as the somewhat stronger ring tilt could be attributed to an increase in the size of the metal center due to the lower oxidation state. The only significant difference in the structure of **2** is the presence of two Li cations connected to the U–ligand moiety through chlorine bridges, as required by the trivalent state of the metal center. NMR spectra were uninformative in this case, showing only very broad resonances. No signals could be observed in the <sup>13</sup>C NMR spectrum.

Further attempts to lower the oxidation state involved reacting tetravalent **1** with a series of reagents (Scheme 1). The outcomes depended greatly on both the reducing agent and reaction conditions. Reaction of **1** with 1 equiv of lithium naphthalenide at 0 °C did not afford **2** but instead yielded a closely related U(III) complex formulated as {1,3-[2,5-(*i*-Pr)<sub>2</sub>PhNC(=CH<sub>2</sub>)<sub>2</sub>C<sub>6</sub>H<sub>4</sub>}U(THF)(μ-Cl)<sub>2</sub>[Li(Et<sub>2</sub>O)<sub>2</sub>] (**3**) (Figure 3). Complexes **2** and **3** differ only in their extents of retention of LiCl. The ligand system showed the same arrangement in the two complexes, forming the same unusual interaction between the metal center and the central aromatic ring. As in the case of **2**, the NMR spectra were uninformative.

Both of the trivalent complexes **2** and **3** reacted thermally in boiling THF, affording oxidation of the metal center to

give the new tetravalent compound {1,3-[2,5-(*i*-Pr)<sub>2</sub>PhNC(=CH<sub>2</sub>)<sub>2</sub>C<sub>6</sub>H<sub>3</sub>}U(THF)(μ-Cl)<sub>2</sub>[Li(THF)<sub>2</sub>] (**4**), in which the oxidation of the trivalent center occurred at the expense of the central phenyl ring C–H bond (Scheme 1). The fate of the hydrogen atom is unclear, since no hydrogen gas was recovered from the reaction when the thermolysis was carried out in a closed vessel connected to a Toepler pump. Also, no significant distortions in the complex that might indicate the presence of a hydride could be observed (Figure 4). As a result of the metalation, the ring becomes almost coplanar with the uranium center, with the small deviation of the metal from the plane probably resulting from the steric repulsion between the *i*-Pr substituents and the coordinated THF molecule. Despite the line broadening, the <sup>1</sup>H NMR spectrum of complex **4** allowed recognition of all of the functional groups of the ligand system. The most striking spectral feature is the significant line separation for the two nonequivalent =CH<sub>2</sub> protons of the two ene-amino moieties, which are also magnetically nonequivalent. These resonances are present as a pair of doublets at 7.17 and 7.13 ppm coupled to other doublets at 2.18 and 2.16 ppm, respectively. The four *i*-Pr substituents give two distinctive doublets centered at 1.47 and 1.44 ppm with the correct integration. These resonances are coupled to two broad multiplets of the corresponding ipso hydrogens located at 3.09 ppm and 7.33 ppm, respectively, with proper integration. The large difference in the chemical shifts is not particularly surprising, given the very different structural environments experienced by these hydrogen atoms. In fact, two are oriented against the coordinated THF molecules while the other two point against a void space. The resonances of the three aromatic rings are located in the conventional range between 9.0 and 7.4 ppm.

The ready ring metalation accompanied by the one-electron oxidation of the metal center under thermal conditions clearly frustrated the possibility of using π coordination to the phenyl ring for possible stabilization of the lower oxidation states. Therefore, further attempts to prepare reduced complexes focused on the use of **1** as the most convenient starting material. In carrying out reduction reactions, we compensated for the consumption of the reductant by the seemingly unavoidable ring metalation through the use of larger stoichiometric ratios.

Reaction of **1** with 3 equiv of lithium naphthalenide at room temperature afforded {1,3-[2,5-(*i*-Pr)<sub>2</sub>PhNC(=CH<sub>2</sub>)<sub>2</sub>C<sub>6</sub>H<sub>3</sub>}U(μ-Cl)(μ-[O(CH<sub>2</sub>)<sub>3</sub>CH<sub>2</sub>])[Li(DME)]<sub>2</sub>[Li(DME)<sub>3</sub>] (**5**) (Scheme 1). In this species, the tetravalent metal center forms a six-membered metallacycle ring with a moiety arising from THF ring opening (Figure 5). Similar ring opening has been observed previously by Burns as the result of a nonredox insertion reaction of THF into U–I bonds.<sup>9a</sup> In the present case, however, the

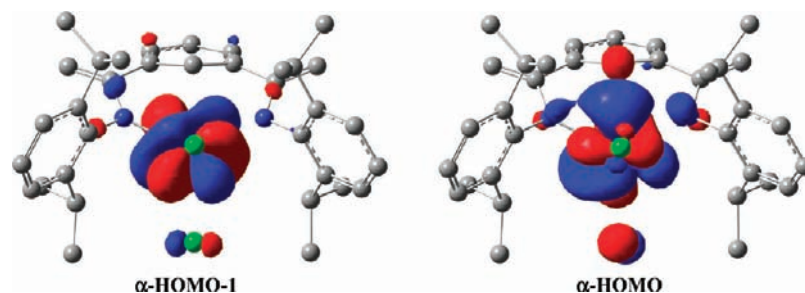
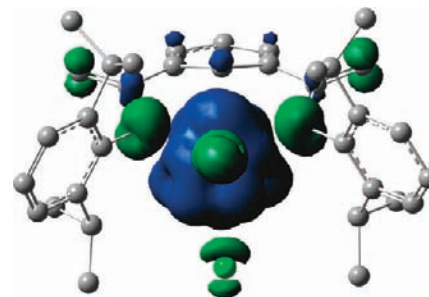


**Figure 10.**  $\alpha$ -HOMO and  $\alpha$ -HOMO-1 orbitals for the optimized structure of complex **1**.

ring opening is clearly the result of two-electron reductive cleavage of the THF O–C bond. Since complex **5** contains tetravalent uranium, it is tempting to state that a transient divalent synthon or reduced species was responsible for the attack. The two ene–amido moieties remained unmodified during the reduction, while ring metalation occurred instead, as expected. The  $^1\text{H}$  NMR spectrum showed all of the aromatic resonances located between 9.14 and 7.05 ppm. The four isopropyl groups displayed only one doublet at 1.15 ppm coupled to a broad multiplet at 2.77 ppm with the expected integration. As in compound **4**, the protons of the ene–amino moiety are magnetically nonequivalent, resulting in a large splitting of one pair of broad signals at 7.19 and 6.87 ppm, respectively. The metallacycle  $-\text{CH}_2-$  groups appeared as four distinct broad resonances. Two of these, tentatively assigned to the U– $\text{CH}_2-$  and U–O– $\text{CH}_2-$  groups, experience the most significant chemical shifts, to  $-6.62$  and  $-4.36$  ppm respectively. The other two  $-\text{CH}_2-$  groups were instead located in the more normal range at 2.17 and 0.98 ppm.

Overall, the THF ring opening and phenyl ring metalation that occurred during the formation of **5** required a total of three electrons, assuming that the aromatic-ring H atom was either released as hydrogen gas or transferred to some other acceptor. To better clarify this point, the same reaction was carried out in a sealed vessel connected to a Toepler pump, but not even a trace of hydrogen gas was produced during the reaction. In addition, the fact that the reaction actually consumed 3 equiv of reductant and both the starting material and final product contain the uranium metal in the tetravalent state clearly suggested that a byproduct may have been formed. To remove the interference from THF cleavage, an identical reduction was performed in the more robust solvent DME. Reduction of **1** in DME with 2 equiv of potassium naphthalenide at room temperature afforded a mixture of two compounds having very similar structure. The two different species,  $[\{1,3\text{-}[2,5\text{-}(i\text{-Pr})_2\text{PhNC}(\text{=CH}_2)]_2\text{C}_6\text{H}_3\}\text{UCl}(\text{OCH}_3)][\text{Li}(\text{DME})_3]$  (**6a**) and  $[\{1,3\text{-}[2,5\text{-}(i\text{-Pr})_2\text{PhNC}(\text{=CH}_2)]_2\text{C}_6\text{H}_3\}\text{UCl}_2][\text{Li}(\text{DME})_3]$  (**6b**), cocrystallized in a ratio very close to 1:1 in the same unit cell, providing single crystals of mixed composition (Figure 6a,b). The salient characteristic of the structure of the two compounds is again the ring metalation, as observed in the previously reported compounds. While complex **6a** has one chlorine atom and one methoxy group, complex **6b** bears two chlorine atoms. The methoxy group is likely generated by DME cleavage, and the uranium is tetravalent in both species. In line with the previous case, no gaseous hydrogen gas was produced during the reaction.

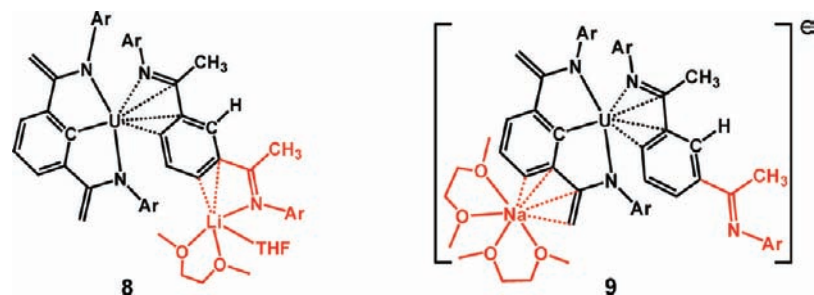
Recent findings have shown that NaH may be a convenient reductant for the preparation of formally low-valent complexes,<sup>17b,18,19d,21</sup> including examples of dinitrogen fixation.<sup>18,19d,21</sup>



**Figure 11.** Spin density distribution for the optimized structure of complex **1**. The isosurface contour value is  $0.0008 \text{ e } \text{\AA}^{-3}$ .

We thus attempted the reduction of **1** with excess of NaH in DME. After a slow reaction, a new species formulated as  $\{1,3\text{-}[2,5\text{-}(i\text{-Pr})_2\text{PhNC}(\text{=CH}_2)]_2\text{C}_6\text{H}_3\}\text{U}(\mu\text{-OCH}_3)_3(\mu,\eta^6\text{-Na})[\eta^3\text{-Na}(\text{DME})]$  (**7**) was isolated in significant yield. Once again, the crystal structure revealed the presence of several methoxy groups coordinated to the U center in addition to the metalation of the ligand phenyl ring (Figure 7). The formation of **7** unfolds some interesting aspects of the reduction process. The formation of a methoxy moiety from DME as the result of the attack by one or two low-valent metal centers was also observed in the case of **6a** and **6b**. The presence of three methoxide units in **7** raises two different possibilities. The first consists of the formation of an “over-reduced” species followed by simultaneous or consecutive “three-step, two-electron oxidations”. Such a large storage of electrons is clearly an improbable event. Perhaps more realistic is a process involving one-electron reduction immediately followed by DME attack, which is repeated three times in what is reminiscent of the beginning of a catalytic process.  $^1\text{H}$  NMR data for **7** showed the usual features. All of the aromatic signals were very well resolved and located between 8.68 and 6.93 ppm. The ene–amino protons showed the enhanced magnetic nonequivalency, with two doublets centered at 7.93 and 7.84 ppm coupled to two other doublets at 2.90 and 2.34 ppm, respectively. The four isopropyl groups displayed two doublets centered at 1.11 and 1.09 ppm coupled to the same multiplet at 2.74 ppm. The positions of the methoxy residue resonances are rather unusual: two of the three methoxy groups gave a broad resonance at  $-3.10$  ppm, while the third was observed as a sharper line at 4.60 ppm.

From the seemingly ubiquitous solvent cleavage and ring metalation, it became apparent that milder reaction conditions were the only possible way to isolate intermediate reduced species of such a high reactivity. Thus, reduction of **1** was carried out at low temperature ( $-35$  °C) with a larger amount of lithium naphthalenide (4 equiv). After suitable workup, the new species  $\{[\{1,3\text{-}[2,5\text{-}(i\text{-Pr})_2\text{PhNC}(\text{=CH}_2)]_2\text{C}_6\text{H}_3\}\text{U}\{1,3\text{-}[2,5\text{-}(i\text{-Pr})_2\text{PhN}=\text{C}(\text{CH}_3)]_2\text{C}_6\text{H}_4\}][\text{Li}(\text{DME})(\text{THF})]\} \cdot \text{Et}_2\text{O}$  (**8**) was

Scheme 3. Simplification of the Structures of Complexes **8** and **9**<sup>a</sup>

<sup>a</sup> Truncated parts are depicted in red. The fragments shown in black were used in the electronic structure analysis.

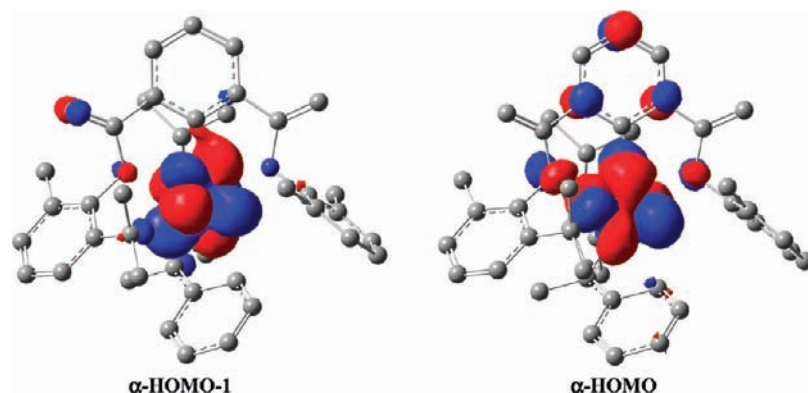


Figure 12.  $\alpha$ -HOMO and  $\alpha$ -HOMO-1 orbitals for the optimized structure of the simplified model of complex **8**.

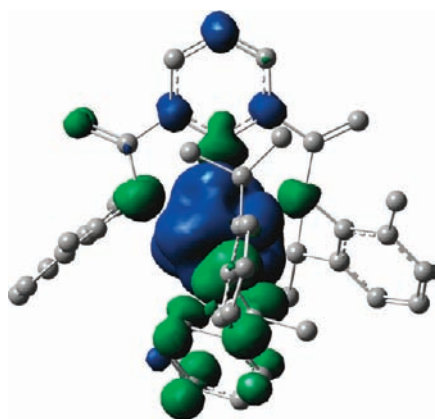
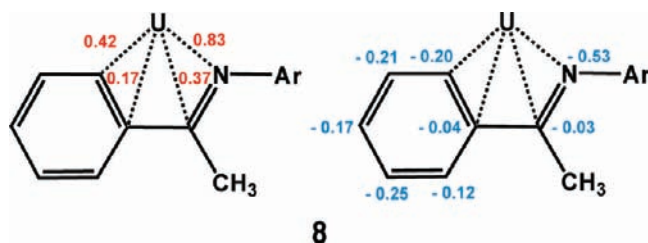


Figure 13. Spin density distribution for the simplified model structure of complex **8**. The isosurface contour value is  $0.0008 \text{ e } \text{\AA}^{-3}$ .

Scheme 4. Mayer Bond Orders (in Red) and MPA-Derived Atomic Charges (au, in Blue) for the  $\pi$ -Bonded Bis(imino)benzene Fragment in **8**



isolated in significant yield (Scheme 2). Even in this case, the uranium atom is surrounded by the much-expected trianionic, ring-metalated ligand (Figure 8). However, a second ligand unit is bonded to the metal center through a part of the  $\pi$  system.

Inspection of the structural parameters clearly indicated that *this second ligand unit has acquired two hydrogen atoms* and that the imine functions have been restored, forming a neutral bis(imino)benzene unit. The formation of complex **8** by reduction of tetravalent **1** is the result of a complex series of transformations. In fact, the presence of one intact *neutral* ligand implies that during the reaction, one doubly deprotonated ligand regained the two hydrogen atoms and then became demetalated and  $\pi$ -coordinated to a second, “*formally reduced*” metal center. While the fate of the demetalated metal center remains unclear, the origin of the two hydrogen atoms can be tentatively ascribed to the phenyl rings of two other ligand units that were phenyl-metalated. Thus, it is possible that ring metalation is not the result of a direct redox transformation but instead arises from a C–H  $\sigma$ -bond metathesis process. In turn, this may explain the absence of hydrogen gas from the reaction mixtures. While this implies that even more uranium-containing species may be partner products of this series of transformations, we observe that from the *formal* point of view, this reaction can be interpreted as a two-electron reduction affording a “*formally*” U(II) bis(amino)benzene complex. Of course, given the  $\pi$  coordination of the additional neutral ligand, the oxidation state is likely to be higher (see below). <sup>13</sup>C NMR data did not provide any useful information because of the very large extent of peak broadening and overlap. The only recognizable features in the <sup>1</sup>H NMR spectrum between +26 and –90 ppm were the methyl signals of the isopropyl group located in their normal positions at 1.29 and 1.85 ppm.

Even though complex **8** gives no evidence of having been directly involved in solvent cleavage, another reduction was carried out at ambient temperature but in noncoordinating solvent. Reaction of **1** with excess NaH in toluene proceeded slowly at room temperature and afforded a significant yield of  $\{[1,3\text{-}[2,5\text{-}(i\text{-Pr})_2\text{PhNC}(=\text{CH}_2)]_2\text{C}_6\text{H}_3\}\text{U}\{1,3\text{-}[2,5\text{-}(i\text{-Pr})_2\text{PhN}=\text{$

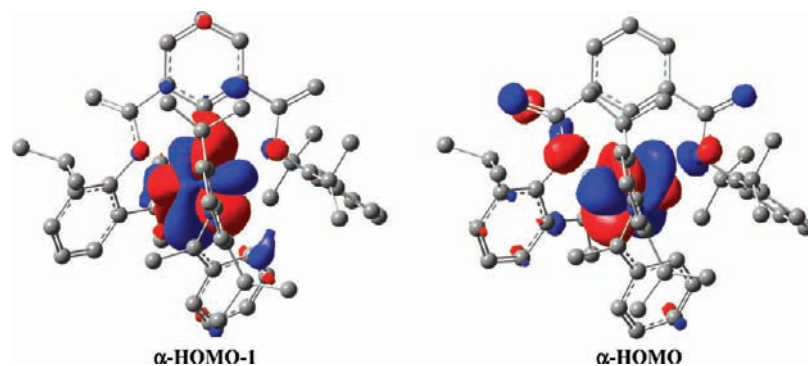


**Figure 14.**  $\alpha$ -HOMO and  $\alpha$ -HOMO–1 orbitals for the optimized structure of the simplified model of complex **9**.

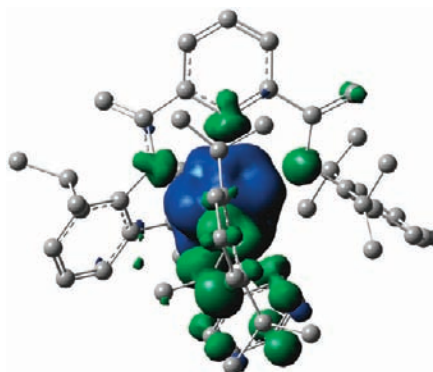
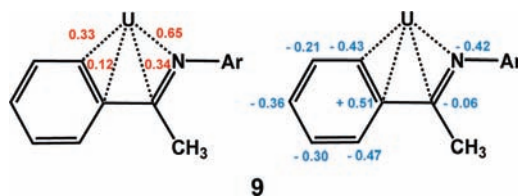


**Figure 15.** Spin density distribution for the simplified model structure of complex **9**. The isosurface contour value is  $0.0008 \text{ e } \text{\AA}^{-3}$ .

**Scheme 5.** Mayer Bond Orders (in Red) and MPA-Derived Atomic Charges (au, in Blue) of the  $\pi$ -Bonded Bis(imino)benzene Fragment in **9**



$\text{C}(\text{CH}_3)_2\text{C}_6\text{H}_4\{\text{Na}(\text{DME})_2\}[\text{Na}(\text{DME})_3] \cdot \frac{1}{2}\text{C}_7\text{H}_8$  (**9**) after crystallization from DME. Similar to **8**, the complex still contains one ring-metalated trianionic ligand and one intact ligand with the H atoms regained and the two imine functions restored (Figure 9). The metric parameters of the anionic moiety in **9** compare well with those of **8**. The main difference consists of the presence of *two* solvated Na atoms instead of *one* Li cation. This assigns a *formal* monovalent state to uranium. Such a low oxidation state is of course unrealistic for uranium, which most likely embarks in a substantial back-bonding interaction with the  $\pi$  system of the neutral ligand. In any event, this complex appears to be a species reduced to the largest extent observed to date. The NMR data for this compound were completely uninformative because of substantial line broadening and signal overlap. Although **8** and **9** are formally highly reduced species, the reactivity of the metal center seems to have been substantially quenched by the acquisition of the second ligand system. These species no longer reacted with ethers and upon exposure to a wide range of mild oxidating agents at high temperature gave only intractable materials.

**Electronic Structures.** The X-ray structures of complexes **1–3** revealed the presence of a close contact between the U metal center and the C–H bond of the central phenyl ring of the ligand. At first glance, the relative positions of these three atoms may suggest the presence of a three-center, two-electron agostic U–H–C interaction. However, DFT calculations performed using the crystallographic atomic coordinates revealed a rather different scenario. A full-molecule geometry optimization was performed prior to the electronic structure evaluation and provided a satisfactory match with the X-ray structural data for all of the bonds and angles (see the Supporting Information).

The calculations established that the three-center bond-order index for the U–C–H interaction in complex **1** is equal to 0, which rules out the presence of agostic interactions. Furthermore, the calculations predicted only a minor elongation of the C–H bond from 1.094 to 1.103 Å, which is smaller than the typical +0.07 Å C–H bond expansion normally expected for a metal–H–C agostic interaction.<sup>32</sup> Accordingly, the U–H bond order is only 0.07. Conversely, the U–C interaction was calculated to be much stronger, displaying a Mayer bond order of 0.23. Such an interaction may be described in terms of weak  $\pi$  bonding and an electron density transfer of 0.06 from the portion of the  $\pi$  orbital located over C8 to the U(IV) atom. The spin density on the U atom was calculated as 2.22, which reveals the presence of two unpaired 5f electrons (Figures 10 and 11). The uranium valence index of 6.9 supports this assumption, indicating the existence of two free valences in addition to five conventional  $\sigma$  bonds.

DFT calculations were also performed on both **8** and **9** to evaluate the most realistic oxidation state of the metal center. From the formal point of view, the two compounds contain the U metal center in the unrealistically low U(II) and U(I) oxidation states, respectively. Both **8** and **9** possess two ligand systems. In each compound, the two ligands bonded to the metal have conceptually different electronic structures. One possesses three negatively charged donor atoms coordinated to the U metal center through three  $\sigma$  bonds. The other displays structural parameters typical of the neutral molecule and is connected to the U metal center through a series of  $\pi$  interactions. In complex **8**, the same  $\pi$ -coordinated ligand system also hosts an alkali cation (Scheme 3). This alkali cation is retained through several  $\pi$  interactions and is situated on the remote part of the ligand system, having no significant interactions with U metal center. Therefore, in

(32) Brookhart, M.; Green, M. L. H.; Parkin, G. *Proc. Natl. Acad. Sci. U.S.A.* **2007**, *104*, 6908.

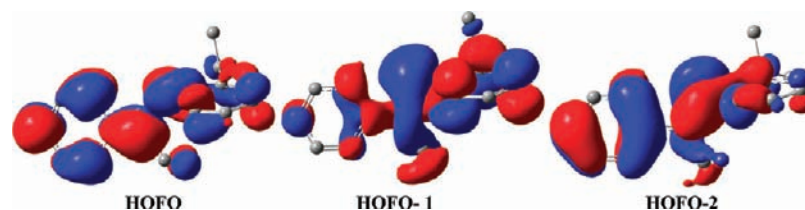


**Figure 16.** Highest-occupied fragment orbitals (HOFOs) of the dianionic ligand that interact with the U(IV) ion in complex **8**.

order to optimize calculation time for compounds **8** and **9**, the calculations were performed on truncated models obtained by replacing the distant half of the bis(imino)benzene molecules by hydrogen atoms. Such a simplification is justified in light of the remote position of this moiety, resulting in total absence of any interaction with U metal center. The geometry of the ligands in both cases prevents extensive conjugation as well as delocalization of the electrons through  $\pi$ -system interactions. It should be also taken into consideration that employing this simplification led to the removal of the alkali cation associated with the truncated part of the molecule in the case of compound **8**. Such cation removal causes the appearance of one additional negative charge on the model structure, for which the presence of the positively charged metal center compensates in the full structure.

Another model simplification involved replacing three out of the four *i*-Pr groups in complex **8** with H atoms. The last *i*-Pr group was not simplified because of its close proximity to the U metal center and possible influence in stabilization of the oxidation state through agostic interactions. All of the *i*-Pr substituents in the model of **9** were preserved for similar reasons. All of the alkali cations and their coordinated solvent molecules were removed from both structures. All of the other heavy-atom coordinates were imported directly from the X-ray data and used without further geometry optimization. All of the C–H bond distances were set to a length of 1.08 Å.

Calculations were performed for different multiplicities corresponding to hypothetical U(II)  $f^4$  and U(IV)  $f^2$  configurations for complex **8** and U(I)  $f^5$  and U(III)  $f^3$  configurations for complex **9**. For complex **8**, the possibilities of singlet ( $S = 0$ ), triplet ( $S = 1$ ), and quintet ( $S = 2$ ) states were evaluated. The results clearly indicated that the triplet state is the ground state for **8**, in further agreement with the strong paramagnetism already suggested by the NMR data. For complex **9**, three possibilities were analyzed, namely, the doublet ( $S = 1/2$ ), quartet ( $S = 3/2$ ), and sextet ( $S = 5/2$ ) ground states. The calculations indicated that the doublet ground state has the lowest total electronic energy, with  $\Delta E_{\text{tot}} = 152.4$  and 23.8 kcal/mol required to reach the quartet and sextet states, respectively. The net electron spin densities on the uranium metal center were determined to be 2.24 for complex **8** and 1.27 for complex **9**. Mulliken population analysis (MPA) for compound **8** revealed two unpaired electrons with nearly pure 5f character (91 and 94% for the  $\alpha$ -spin HOMO and HOMO–1, respectively; Figure 12), accounting for the spin density distribution shown in Figure 13. In summary, the most realistic oxidation state of the uranium center in this species can be assigned as +4, with the ligand molecule playing the role of storage of electron density. The electrons hosted in the  $\pi$ -bonded ligand fragment are used for diene-ty bonding with the U metal center (Scheme 4).

Similar to complex **8**, MPA of **9** indicated that the complex has three electrons in three nearly degenerate U 5f nonbonding orbitals (89% U for the  $\alpha$ -HOMO, 92% U for the  $\alpha$ -HOMO–1, and 100% U for the  $\beta$ -HOMO; Figure 14), resulting in the spin density distribution shown in Figure 15. In this case, the most realistic oxidation state of the metal center could be regarded as +3, with the ligand hosting two “additional” electrons in the delocalized  $\pi$  system as presented in Scheme 5.

Calculations on the  $\pi$ -bonded moiety holding an overall charge of –2 indicated that for complex **8** as well as complex **9**, two additional electrons are hosted mainly in the three highest-occupied fragment orbitals (HOFOs) of the  $\pi$ -coordinated ligand (Figure 16).

Overall, the donor–acceptor interactions between the uranium ion and the dianionic  $\pi$ -bonded moiety in complex **8** are limited to charge transfer to the metal from the HOFOs in Figure 16. This charge transfer is evident from the changes in the orbital occupancies upon complex formation:<sup>28c</sup>  $\alpha$ -HOFO, 40.4%;  $\beta$ -HOFO, 27.2%;  $\alpha$ -HOFO–1, 13.3%;  $\beta$ -HOFO–1, 11.3%;  $\alpha$ -HOFO–2, 13.1%;  $\beta$ -HOFO–2, 11.4%. As can be seen from the changes in occupancies, the HOFOs of the ligand play the most important role in charge transfer to the U(IV) ion. Since the nature of these orbitals in complexes **8** and **9** is nearly identical, the same orbitals contribute to covalent bonding between the metal and the ligand in complex **9**:  $\alpha$ -HOFO, 43.0%;  $\beta$ -HOFO, 26.6%;  $\alpha$ -HOFO–1, 14.1%;  $\beta$ -HOFO–1, 11.4%;  $\alpha$ -HOFO–2, 12.1%;  $\beta$ -HOFO–2, 10.2%. These large changes in the donor-orbital occupancies highlight the importance of metal–ligand covalent interactions in the stabilization of **8** and **9**.

The most significant observed difference between **8** and **9** involves the interactions of the metal center with the aliphatic carbons of the isopropyl groups. In the case of **8**, such interactions are completely negligible. However, in the case of **9**, several of the C–H bonds of the isopropyl groups are oriented to interact with the U atom, with one ipso C–H interaction being noticeably stronger. The significance of these interactions is confirmed by the Mayer bond orders for the corresponding U–C and U–H contacts, for which the largest values (0.35 and 0.21, respectively) were found for U1–C32 and U1–H32a. Although they contribute to the stabilization of the complex, these interactions do not cause significant changes in the C–H bond lengths.

## Conclusions

Use of the bis(imino)benzene ligand made possible the isolation of several new U complexes. Reduction reactions mainly led to different solvent fragmentation products. In every case, the solvent fragmentation suggested transient formation of low-valent or reduced species. In contrast, the ligand system appears to be quite resilient, as its only involvement in the reactivity of the metal center is the direct metalation of the aromatic ring. Decreasing the temperature of the reduction or using noncoordinating solvents

allowed the isolation of two complexes in which the U metal center coordinates to two anionic radical ligands. In these species, the metal center deceptively appeared to be unusually low-valent. However, DFT calculations unequivocally confirmed that the actual oxidation states of the U metal centers in these two complexes could be assigned as U(IV) and U(III), respectively, and that the U centers were coupled to dianionic forms of the ligand, with electron storage performed by the  $\pi$ -coordinated systems.

**Acknowledgment.** This work was supported by the Natural Science and Engineering Research Council (NSERC) of Canada.

**Supporting Information Available:** Complete ref 24, crystallographic data (CIF), and tables of computational data. This material is available free of charge via the Internet at <http://pubs.acs.org>.

JA9002525